12-2016

Evaluation of Smart Water Flooding In a Selected UAE Carbonate Oil Reservoir

Mohammad Jasem Khalifi

UAEU

جامعة الإمارات العربية المتحدة
United Arab Emirates University

United Arab Emirates University

College of Engineering

Department of Chemical and Petroleum Engineering

EVALUATION OF SMART WATER FLOODING IN A SELECTED UAE CARBONATE OIL RESERVOIR

Mohammad Jasem Khalifi

This thesis is submitted in partial fulfilment of the requirements for the degree of Master of Science in Petroleum Engineering

Under the Supervision of Professor Abdulrazag Y. Zekri

December 2016

Declaration of Original Work

I, Mohammad Jasem Khalifi, the undersigned, a graduate student at the United Arab Emirates University (UAEU), and the author of this thesis entitled *"Evaluation of Smart Water Flooding in a Selected UAE Carbonate Oil Reservoir"*, hereby, solemnly declare that this thesis is my own original research work that has been done and prepared by me under the supervision of Professor Abdulrazag Y. Zekri, in the College of Engineering at UAEU. This work has not previously been presented or published, or formed the basis for the award of any academic degree, diploma or a similar title at this or any other university. Any materials borrowed from other sources (whether published or unpublished) and relied upon or included in my thesis have been properly cited and acknowledged in accordance with appropriate academic conventions. I further declare that there is no potential conflict of interest with respect to the research, data collection, authorship, presentation and/or publication of this thesis.

Student's Signature: _____   Date: 12/12/2016

Advisory Committee

1) Advisor: Dr. Abdulrazag Y. Zekri

Title: Professor

Department of Chemical and Petroleum Engineering

College of Engineering

2) Co-advisor: Dr. Hazim Al Attar

Title: Associate Professor

Department of Chemical and Petroleum Engineering

College of Engineering

Approval of the Master Thesis

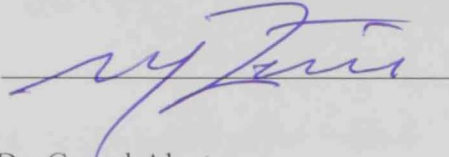This Master Thesis is approved by the following Examining Committee Members:

1) Advisor (Committee Chair): Dr. Abdulrazag Y. Zekri

   Title: Professor

   Department of Chemical and Petroleum Engineering

   College of Engineering

   Signature _____   Date _24/11/2016_
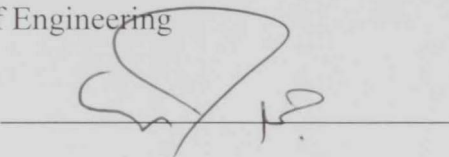
2) Member: Dr. Gamal Alusta

   Title: Assistant Professor

   Department of of Chemical and Petroleum Engineering

   College of Engineering

   Signature _____   Date 24/11/2016
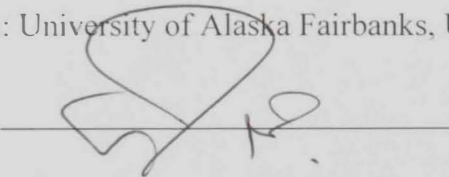
3) Member (External Examiner): Dr. Shirish Patil

   Title: Professor

   Department of Petroleum Engineering

   Institution: University of Alaska Fairbanks, USA

   Signature _____   Date 24/11/2016

This Master Thesis is accepted by:

Dean of the College of Engineering: Professor Sabah Alkass

Signature _____ Date 12/12/2016

Dean of the College of the Graduate Studies: Professor Nagi T. Wakim

Signature _____ Date 13/12/2016

Copy 5 of 6

Abstract
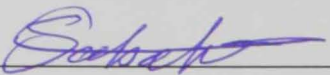
Water flooding is by far the most common method of improved oil recovery applied in oil reservoirs. Water is the cheapest source of external energy that has been used over decades in water flooding schemes, provided that the formation damage does not adversely affect its injectivity. Displacement efficiency of water flooding can be significantly affected by crude oil/water/rock interactions. Historically, some consideration was given to such interactions in the practice of reservoir engineering. In recent years, extensive research in this area has documented that higher oil recoveries can be obtained when low-salinity water is injected in a formation with high salinity formation water. Hence, selecting a "smart water" with the proper salinity and ionic composition could be considered as a tertiary recovery fluid. While laboratory tests and historical field evidences validated this observation in carbonate reservoirs, the mechanism behind the observed incremental increase of oil recovery is still a topic of discussion. In this work, selected core samples from a carbonate reservoir were used to run flooding and spontaneous imbibition experiments at reservoir temperature and a potential smart water that could yield maximum oil recovery has been identified. Measurements of endpoint effective permeabilities along with chemical analysis of the effluents at the end of each core flooding test were employed to suggest the likely mechanism for the incremental increase of oil recovery.

Keywords: Low-Salinity, Smart Water, Core Flooding, Amott, IFT, Contact Angle.

Title and Abstract (in Arabic)

تقييم ألأفاضه بالماء الذكي في احد المكامن النفطيه المختاره في دولة ألأمارات ألعربيه المتحده

الملخص

تعتبر تقنية حقن المياه من أكثر التقنيات ٠ عا لتحسين استخراج النفط من خزانات النفط. تعد المياه من أرخص مصادر الطاقة الخارجية التي استخدمت على مدى عقود من الزمن في تقنية حقن المياه .كفاءة تقنية إحلال المياه مكان النفط يمكن أن تتأثر بشكل كبير من التفاعلات بين النفط و المياه و الصخور الخام. تاريخيا، أ ٠٠ت بعض هذه التفاعلات بعين الاعتبار في ممارسة هندسة خزانات النفط. في السنوات الأخير ، أكدت الأبحاث المكثفة في هذا المجال أنه يمكن استخراج النفط بكميات كبيرة عن طريق حقن المياه قليلة الملوحة بالإضافة إلى مياه عالية الملوحة لتكوين ما يسمى بالمياه الذكية. اختيار "المياه الذكية" مع الملوحة والمكونات الأيونية المناسبة يمكن يعتبر ك السوائل الانتعاش العالي. على الرغم من أن الفحوصات المخبرية والأدلة الميدانية التاريخية قد تحققت من صحة هذه الملاحظة عن طريق خزانات الكربونات، إلا أن آلية الزيادة التدريجية في استخراج النفط مازالت موضوعا للمناقشة. تناقش هذه الرسالة استخراج عينات مختارة من خزانات الكربونات لإجراء تجارب متعلقة بالحقن و الامتصاص اللحظي باعتماد درجة حرارة الخزان و استخدام المياه الذكية التي أسفرت عن استخراج أعلى كميات للنفط . تم توظيف قياسات النفاذية جنبا إلى جنب مع التحليل الكيميائي للمياه الصرف في نهاية كل اختبار للحقن لاقتراح آلية لزيادة استخراج النفط.

مفاهيم البحث الرئيسيه: قليل الملوحة، الحقن الأساسي، التوتر الصحي، Amott، زاوية الاتصال.

Acknowledgements

Firstly, I would like to express my sincere thanks and gratitude to my advisor Prof. Abdulrazag Zekri and my co-supervisor Dr. Hazim Al Attar for their continuous support, constructive advice and encouragement throughout this work. I would like to thank my all professors for their effort and support during my bachelor program which helped me build a solid background in petroleum engineering. My special thanks goes to Dr. Hazim Al Attar who taught me various core courses in reservoir and production engineering throughout my bachelor and masters studies.

I would also like to thank the Graduate program coordinator, Dr. Gamal Alusta for his significant support and assistance throughout my MSc program and the different phases of my thesis. My appreciation also goes to all the faculty and staff of the chemical and petroleum engineering for their precious support and encouragement. I would like to extend my special gratitude to my colleague Eng. Jassim Abubacker Ponnambathayil for his valuable work in the first phase of this project. In addition, special thanks are extended to the faculty and staff in the Geology Department for their great help and effort during my experimental work.

Finally, I would like to thank my parents for the support and encouragement that motivated me and helped me to overcome the obstacles I have faced during my graduate career.

Dedication

To my beloved parents and family

Table of Contents

List of Tables

List of Figures

List of Abbreviations/Nomenclatures/Symbols

A	Area of the core plug
ADCO	Abu Dhabi Company for Onshore Petroleum Operations
ADNOC	Abu Dhabi national oil company
C_1	Concentration of the seawater
C_2	Concentration of the injected brine
CA	Contact angle
E	Displacement efficiency
E_D	Microscopic displacement efficiency
E_V	Macroscopic displacement efficiency
FW	Formation water
HTHP	High temperature and high pressure conditions
IFT	Interfacial tension
I_o	Oil saturation index
IW	Injection water
I_w	Water saturation index
K	Permeability
K_a	Absolute permeability
K_{eff}	Effective permeability
L	Length of the core plug
LSWF	Low salinity water flooding
OIIP	Oil initially in place
PV	Pore volume
Q	Injection rate

S_{oi}	Initial oil saturation
SW	Seawater
S_{wirr}	Irreducible water saturation
V_1	Required volume of the seawater
V_2	Required volume of the injected brine
V_{oi}	Initial volume of oil
$V_{p.oil}$	Cumulative volume of the produced oil
V_{water}	Cumulative volume of the produced water
ΔP	Change in pressure

Chapter 1: Introduction

1.1 Overview

Energy demand is increasing with the rise in the world's population. Based on IEO2016 report, the total world energy consumption demand is expected to increase by 48%, from 549 quadrillion British thermal units (Btu) in 2012 to 815 quadrillion Btu in 2040. Despite the significant advances in renewable energy technologies, fossil fuels will continue to provide most of the world's energy. In 2040 fossil fuels are expected to account for about 78% of the world's total energy consumption. Population growth and fast-paced economic development in the Middle East would result in a 95% increase in the region's energy consumption by 2040 (International Energy Outlook, 2016).

As oil and gas will continue to be the main energy source in the Middle East, increases in production and development of the fields will be paramount with an emphasis on more efficient production techniques, both financially and technically

1.2 Background

Oil recovery operations are technically subdivided into three stages: primary, secondary, and tertiary/EOR. The production life of a field can be divided into different phases, mainly based on the reservoir pressure and the natural energy available. Historically, these phases have been applied in a sequential manner (Green & Willhite, 1998). In the initial stages of the production life of a reservoir, fluids are usually produced naturally (or with the help of artificial lift methods) through the wellbore. The continuous fluid withdraw from the reservoir would result in reduction of the reservoir pressure, unless it is supported by a strong water aquifer. Economically

feasible secondary/tertiary recovery methods are then applied to produce the oil at the required production rate.

1.2.1 Primary Recovery

During the primary recovery, initial production is done with natural drives of the reservoirs. Natural drives may include: a natural aquifer displacing the oil toward the wellbore, expansion of the fluids already in the reservoir, compaction of the pore space, gravity segregation of fluids with different densities and expansion of the gas cap overlaying the oil accumulation. Depending on the combination and strength of the natural drives of a reservoir, the oil recovery during the primary stage can range from typically 5-25% of Oil Initially in Place (OIIP) in depletion drive reservoirs (Tzimas, Georgakaki, 2005) and 15-50% in black oil reservoirs with a water drive mechanism (Arps, J. J., 1967).

1.2.2 Secondary Recovery

In most cases, the production under a natural drive would result in a reservoir pressure drop. Having lower reservoir pressure may prevent meeting the production targets, or increase the gas to oil ratio of the production. Thus, secondary recovery methods are applied after exhausting the natural potential of the reservoir. In secondary recovery techniques, water or immiscible gases are injected in the reservoir to maintain the reservoir pressure above a predefined limit.

Water flooding is by far the most commonly practiced secondary recovery technique that is used to enhance and accelerate oil recovery. This is why nowadays, secondary oil recovery is synonymous with to water flooding (Green & Willhite, 1998). In addition to pressure maintenance by means of voidage displacement, water

flooding can displace the oil from the pore space. The efficiency of this displacement depends on the viscosities of the displacing and displaced fluids, the rock characteristics and gravity. In some cases like Ekofisk field, water flooding can be used to prevent surface subsidence (Dake, 2001).

The overall displacement efficiency of any flooding technique, can be conventionally considered as multiplication of microscopic and macroscopic displacement efficiencies.

$$E = E_D E_V$$

Where E_D as microscopic displacement efficiency is a measure of effectiveness of the displacing fluid in mobilizing the oil. While E_V, or macroscopic displacement efficiency (also referred as sweep efficiency), is a measure of the effectiveness of the displacing fluid in contacting the oil (Green & Willhite, 1998).

Almost without exception, water from the cheapest source is used at the start of water flooding, provided that scaling and formation damage does not affect the injectivity (Robertson, 2007). Historically, little consideration has been given to the effect of water mineral composition on the oil/water/rock interaction. In other words, the microscopic displacement efficiency that is a result of the chemical or physical interactions between fluids and the rock are disregarded.

1.2.3 Tertiary Recovery

Tertiary oil recovery is the third stage of oil recovery that is usually implemented after water flooding (or any other secondary recovery methods that were applied). The tertiary recovery is also referred to as enhanced oil recovery (EOR), as some reservoirs may not follow the common sequential production phases due to

technical and economic factors (Green & Willhite, 1998). In the EOR techniques, physical and/or chemical properties of the rock and fluids are modified to increase the oil recovery. These favorable controlled modifications may increase oil recovery by altering the wettability conditions, reducing the interfacial tension (IFT), changing density or viscosities, etc. In other words, in EOR techniques, microscopic displacement efficiency is the main area of concern. Enhanced oil recovery processes can be categorized in four main subclasses of: chemical/biochemical flooding, mobility control, miscible displacement, and thermal recovery processes(Green & Willhite, 1998).

Choosing the proper EOR technique that can be both feasible and efficient for a specific reservoir is a big challenge and requires extensive studies on the rock, fluids, natural drive mechanism, heterogeneity of the reservoir, and etc. The price and availability of the EOR fluid is also a consideration. Deciding to apply an EOR technique on a major reservoir may require significant amount of EOR fluids. Some EOR processes like CO_2 flooding prove to be very effective in enhancing the oil recovery, but they are subjected to high operational cost and limited supply of EOR fluid (Green & Willhite, 1998). Thus, a successful EOR process would uses injection fluid that can enhance the recovery by utilizing the available resources at a feasible cost.

For fields that have access to a source of water, a fluid that can use water as its base and meanwhile enhances the microscopic displacement efficiency would be a good EOR candidate. Low-salinity water flooding is one of the new EOR techniques that has proved to increase the oil recovery. About 15 years ago, it was observed that greater oil recovery could be obtained when low salinity water was injected in a core that was initially flooded with high salinity water (Sheng, 2014). Low salinity water

flooding is an emerging EOR technique in which the salinity of the injected water is modified to increase the oil recovery as well as maintaining the reservoir pressure. The potential of low salinity water flooding has been validated by many researchers through laboratory experiments (Y

(Robertson, 2007) in both secondary and tertiary recovery stages. Yet, the underlying mechanism is still undefined.

1.3 Statement of the Problem

The Positive effect of low-salinity water flooding has been validated in sandstone formations. The validation has been done through 214 core flooding experiments used to evaluate the potential of low-salinity brines as secondary recovery fluids, and 188 core flooding experiments as tertiary recovery processes (Al-adasani, Bai, & Wu, 2012).

Generally, recovery factors in sandstone reservoirs are higher than that of carbonates. This is due the fact that carbonate reservoirs have more complex texture and pore network that result in challenges in reservoir characterization, production and management (Schlumberger, 2007). Schlumberger market review 2007 shows that carbonate reservoirs hold more that 60% of the world's oil. The Middle East has 62% of the world's conventional oil reservoirs, and approximately 70% of them are carbonates (Schlumberger, 2007).

Although the potential of incremental recovery is higher in carbonate reservoirs, there are few core flooding and imbibition studies that are done in this area (Al-adasani et al., 2012). Recent studies show that low- salinity water flooding can have a positive effect on the oil recovery in carbonates. But there is still no definite

justification for the reason and mechanism behind this phenomenon (Gupta et al., 2011).

1.4 Relevant Literature

Injecting a brine with manipulated ionic composition can increase the oil recovery in both secondary and tertiary core floods (Lager, Webb, Collins, & Richmond, 2008; Yildiz & Morrow, 1996). This hypothesis has been validated for sandstone reservoirs by many authors.

Zhang and Morrow (2006) have examined the potential of low salinity water flooding (LSWF) as a secondary and tertiary recovery technique and compared it with the injection of formation brine. The experiments covered 5 types of Berea sandstones with a wide permeability range of 60 to 1100 mD and three different crude oils. It has been shown that injection of low salinity water as a secondary recovery fluid could increase the oil recovery by 13% to 27% (Y. Zhang & Morrow, 2006).

Al adasani et al. (2012) has conducted a total of 214 core flooding experiments on injecting brines with low salinity as a secondary recovery fluid, and 188 experiments in which low salinity brines where used in the tertiary recovery stage. Almost with no exception, all low salinity brines resulted in more crude oil recovery in sandstone cores. Carbonate formation have greater reserve volumes (Schlumberger, 2007) and would require lower dilution ratios when compared to sandstone reservoirs (Yousef et al. , 2010). Although, carbonate reservoirs are better candidates for low salinity water flooding applications, there are limited imbibition and core flooding studies that have investigated the optimal injected brine composition (Al-adasani et al., 2012).

Bagci et al. (2001), conducted the first low salinity core flooding on carbonate core samples to investigate the effect of monovalent and divalent cations. The results indicated that low salinity water flooding could increase oil recovery, especially in the absence of divalent cations. The experiments were conducted in an initial water-wetting state.

In 2005, the effects of sulfate ion and temperature was studied on chalks (Peimao Zhang & Austad, 2005) and limestone core samples (Hognesen, Strand, & Austad, 2005). The experiments were conducted using the Middle East formation waters, oil samples with a relatively high acid number and rocks in oil-wet state. The results have indicated that increasing sulfate would result in additional recovery. The incremental recovery was obtained by a favorable alteration of the wettability toward more water-wetting state, through a process that was accelerated by the increase in temperature. In the formation brines with high calcium concentration, the addition of sulfate rendered the recovery due to anhydrate precipitation (Strand et al., 2006). The positive contribution of sulfate ion in low salinity water flooding was confirmed by Webb et al. (2005) through the shift in the capillary pressure curve.

A previous study of P. Zhang & Austad (2005) has indicated that the main factor dictating the wettability of a carbonate rock is the acid number (AN). The carboxylic group of the crude oil makes up the acidic components of the oil. They can strongly adsorb onto the chalk surface and significantly alter the wettability conditions. The increasing acid number can alter the wettability from neutral to strongly oil-wet conditions. The study emphasized the importance incorporating acid number into wettability studies.

The effect of decreasing the ion concentration of seawater was investigated by Yousef et al. (2   s

series). Yousef et al. used IFT, contact angle and capillary measurements as a justification for wettability alteration. Further dilutions resulted in a shift in wettability conditions from an intermediate-wetting state to more water-wet conditions. This observation was then used to explain why extreme dilution of seawater could not increase oil recovery

Gupta et al. (2011) has conducted IFT and core flooding experiments to: (a) investigate the effect of polyatomic anions like sulfate, phosphate and borate in the injected water, and (b) study the effect of cation concentrations. The results suggested that injecting seawater has reduced the pressure drop across the core plug and could increase the recovery. An Increase in the polyatomic anions could further increase the oil recovery. Seawater incremental recovery was accompanied by a reduction of calcium and an increase in the potassium concentration. Gupta et al. also observed an improvement in recovery by reducing the calcium concentration.

Al Harrasi et al. (2012) have conducted spontaneous and core flooding experiments at 70 °C on carbonate rocks. Various injected brines were prepared by dilution of the formation brine using distilled water (to 2, 5, 10, and 100 times diluted). The results indicated that low salinity water flooding can increase the recovery by 16-21%.

Zekri et al. (2011) used various dilution of sea water to study the contact angle as a function of time. Carbonate rocks and sandstone core plugs obtained from Libyan oil reservoirs were used for this study. Zekri et al. concluded that injecting low salinity water would result in incremental oil recovery through a wettability alteration

mechanism.

Al-Attar et al. (2013) conducted core flooding experiments using various dilution factors of seawater and carbonate core plugs from Bu Hassa Field in the United Arab Emirates. Additionally, they evaluated the wettability alteration using contact angle and IFT measurements. Al-Attar et al. have concluded that an increment in oil recovery can be observed using low salinity water flooding while extreme dilutions could render this phenomenon. An increase in sulfate concentration showed a significant effect on oil recovery, but no measurement of acid number of the oil was provided. Results also indicated that there is no clear correlation between IFT and pH, and oil recovery improvement.

Austad et al. (2012) conducted core flooding experiments on preserved carbonate reservoir core samples that contained a significant amount of anhydrate ($CaSO4$). Successive core flooding on composite limestone cores was attempted using 2, 10 and 20 times diluted seawater and oil with acid number of 0.15 mg KOH/g. Reducing the salinity and concentration of inactive salts like NaCl, resulted in a reduction of the sulfate concentration in injected brine due to dissolution of anhydrates. The oil recovery increased gradually by 25, 30 and 33% of OOIP after flooding the core successively at 100 °C with formation water, seawater, and 10 times diluted seawater. Both an increase in the sulfate concentration and a reduction in the concentration of inactive salts contributed positively to oil production. Austad et al. suggested anhydride dissolution to be the main mechanism of recovery improvement in rocks with a significant amount of anhydrates.

1.5 Research Objective

The main objective of this research is to find the optimum composition of the injection brine that is both feasible and practical, and would increase the oil recovery. This work also aims to investigate the mechanism behind low-salinity water flooding in carbonate formations. All the rock samples, reservoir fluids and injected brines, and test conditions were selected so that they resemble an actual oil field in the United Arab Emirates. The objectives are achieved by performing the followings:

First: Studying the physiochemical properties of Oil, Rock, Formation water, injection water and seawater.

Second: Studying the interfacial tension (IFT) and contact angles for various low-salinity fluid candidates. This part of work has been conducted at the first phase of the project and the results are presented in the MSc thesis of Eng Jassim AbuBacker (Jassim Abubacker Ponnambathayil, 2016)

Third: Conducting spontaneous imbibition tests (at high temperature) to investigate the potential of various brines in altering the wettability towards more favorable conditions.

Forth: Conducting core flooding experiments at reservoir temperature conditions to find the optimum smart-water under dynamic conditions.

Fifth: Suggesting the possible recovery mechanism by comparing the physiochemical properties of rock and effluents before and after the core flood, and correlating them with IFT and contact angle results.

1.6 Organization of the Thesis

This thesis consists of five chapters. Chapter 1 includes an overview of the energy and oil industry, the background of oil production, a review of the relevant literature, a statement of the problems, and the objectives of the research work.

The second chapter includes an overview about rocks and fluids that were used in this study. The chapter also includes a brief discussion and elaboration of the experiments and the test conditions at which they were conducted.

The third chapter presents the results of the experimental work and the relevant discussions that were driven to conclusions. The chapter starts with the chemical and physical properties of fluids and IFT and the contact angle measurements. The main part of this chapter is the results of the low salinity water flooding experiments and spontaneous imbibition.

The work is then concluded in chapter 4 and a recovery mechanism is suggested.

Chapter 2: Methodology and Materials

2.1 Asab Oil Field

All the fluid samples used throughout the project were either collected from Asab oil field or synthesized based on the compositions provided by Abu Dhabi Oil Company (ADNOC). Asab Field is one of the five major fields operated by Abu Dhabi Company for Onshore Petroleum Operation Ltd (ADCO). This carbonate formation with total proven oil reserve of 3.6 billion barrels was discovered in 1965. The field is located approximately 84 km north west of Abu Dhabi Island in rolling sand dunes some 30 km north of Liwa oasis. Asab oil field is under current oil production rate of approximately 450,000 barrels per day. The current reservoir pressure and temperature of the reservoir are 3100 psia and 255 °F ("The South East," n.d.).

2.2 Crude Oil

Stock tank crude oil samples from Asab field were used in this study. The light Asab crude oil with API of 39.5 was filtered through a 5mm filter paper prior to any lab application. No asphaltene precipitation was observed during the storage. The crude oil had an acid number of 0.07 mg KOH/g, measured using a standard titration procedure of ASTM D664. Oil viscosity was measured using rolling ball viscometer at 20 °C and the value was 2.93 cP. The chemical analysis of the oil was done using gas chromatography and reported in table 3.3.

2.3 Brines

A total number of 26 brines were used in the IFT and contact angle study phases of this project. These brines include the formation water (FW), the water currently

being injected in the reservoir (IW) and seawaters (SW) with different salinity and sulfate concentrations.

The results of IFT and contact angle have shown that the seawater is the most potential smart water to enhance the oil recovery of Asab field (Jassim Abubacker Ponnambathayil, 2016). Thus, the current study mainly focuses on the seawater and its 10 and 50 times dilutions. Testing the sea water and its dilutions at different sulfate spiking was also attempted as sulfate have been proven to be a determining ion in increasing the oil recovery (Gupta et al., 2011; P. Zhang & Austad, 2005). A seawater sample was collected by Abu Dhabi Oil Company from a location 60 km from Asab field in the Persian Gulf and an ionic analysis was performed. Seawater with total dissolved solids (TDS) of 57,539 was selected as the base brine of the study and was synthetically prepared in the laboratory. Different brines were then prepared by diluting the sea water and spiking it with specific amount of sulfate ion. Dilution and spiking calculations and procedures used for brine preparation are presented in Appendix A to C.

Asab Formation water has a TDS of 157,488 with a density of 1.1034 and a viscosity of 1.2482 cp at ambient conditions. The high salinity water currently being injected in the reservoir has a TDS of 258,250 mg/l with a density of 1.1639 mg/l and a viscosity of 1.75 cp at ambient conditions. Brine calculations and synthetic preparation of all the brines were carried out following the procedure presented in appendix A and appendix B, after ionically balancing the brine compositions. Tables 2.2 to 2.5 show the composition of all brines used in this study. To ease the analysis and comparisons, the brines were categorized based on their dilution and sulfate spiking into seven different categories. Brine categories are presented in table 2.1.

Table 2.1: Brine categories

Category 1	Category 2	Category 3	Category 4	Category 5	Category 6	Category 7
FW	SW	SW/10	SW/50	SW	SW2 x2 SO4	SW2 x6 SO4
IW	SW x2 SO4	SW/10 x2 SO4	SW/50 x2 SO4	SW/10	SW2/10 x2 SO4	SW2/10 x6 SO4
SW	SW x6 SO4	SW/10 x6 SO4	SW/50 x6 SO4	SW/50	SW2/50 x2 SO4	SW2/50 x6 SO4

Table 2.2: Compositions of the Category 1 brines

	FW		IW		SW	
Ion	mg/L	ppm	mg/L	ppm	mg/L	ppm
Sodium	44261	44312	72237	72320	19054	19076
Calcium	13840	13856	19763	19786	690	691
Magnesium	1604	1606	3569	3573	2132	2134
Barium	<0.1	<0.1	1039	<0.1	<0.1	<0.1
Potassium	<0.1	<0.1	1859	1861	672	673
Zinc	<0.1	<0.1	<0.1	<0.1	<0.1	<0.1
Phosphate	<0.1	<0.1	5	5	<0.1	<0.1
Chloride	96560	96670	158518	158699	35836	35877
Bicarbonate	332	332	43	43	123	123
Sulphate	885	886	268	269	3944	3949
Strontium	944	<0.1	944	<0.1	<0.1	<0.1
Nitrate	0	<0.1	4	<0.1	<0.1	<0.1
Carbonate	<0.1	<0.1	<0.1	<0.1	<0.1	<0.1
TDS (mg/L)	157482		257206		62451	
Total (ppm)		157662		256551		62522

Table 2.3: Compositions of the Category 2 brines

	SW		SW x2 SO_4^{2-}		SW x6 SO_4^{2-}	
Ion	mg/L	ppm	mg/L	ppm	mg/L	ppm
Sodium	19054	19076	20748	20772	24137	24165
Calcium	690	691	690	691	690	691
Magnesium	2132	2134	2132	2134	2132	2134
Barium	<0.1	<0.1	<0.1	<0.1	<0.1	<0.1
Potassium	672	673	672	673	672	673
Zinc	<0.1	<0.1	<0.1	<0.1	<0.1	<0.1
Phosphate	<0.1	<0.1	<0.1	<0.1	<0.1	<0.1
Chloride	35836	35877	35836	35877	35836	35877
Bicarbonate	123	123	123	123	123	123
Sulphate	3944	3949	5714	5721	9254	9265
Carbonate	<0.1	<0.1	<0.1	<0.1	<0.1	<0.1
TDS (mg/L)	62451		65915		72844	
Total (ppm)		62522		65990		72927

Table 2.4: Compositions of the Category 3 brines

Ion	SW/10		SW/10 x2 SO$_4^{2-}$		SW/10 x6 SO$_4^{2-}$	
	mg/L	ppm	mg/L	ppm	mg/L	ppm
Sodium	1905	1908	2753	2756	5294	5300
Calcium	69	69	69	69	69	69
Magnesium	213	213	213	213	213	213
Barium	<0.1	<0.1	<0.1	<0.1	<0.1	<0.1
Potassium	67	67	67	67	67	67
Zinc	<0.1	<0.1	<0.1	<0.1	<0.1	<0.1
Phosphate	<0.1	<0.1	<0.1	<0.1	<0.1	<0.1
Chloride	3584	3588	3584	3588	3584	3588
Bicarbonate	12	12	12	12	12	12
Sulphate	394	395	2164	2167	5704	5711
Carbonate	<0.1	<0.1	<0.1	<0.1	<0.1	<0.1
TDS (mg/L)	6245		8862		14944	
Total (ppm)		6252		8872		14961

Table 2.5: Compositions of the Category 4 brines

Ion	SW/50		SW/50 x2 SO$_4^{2-}$		SW/50 x6 SO$_4^{2-}$	
	mg/L	ppm	mg/L	ppm	mg/L	ppm
Sodium	381	382	2753	2756	7836	7845
Calcium	14	14	14	14	14	14
Magnesium	43	43	43	43	43	43
Barium	<0.1	<0.1	<0.1	<0.1	<0.1	<0.1
Potassium	13	13	13	13	13	13
Zinc	<0.1	<0.1	<0.1	<0.1	<0.1	<0.1
Phosphate	<0.1	<0.1	<0.1	<0.1	<0.1	<0.1
Chloride	717	718	717	718	717	718
Bicarbonate	2	2	2	2	2	2
Sulphate	79	79	1849	1851	5389	5395
Carbonate	<0.1	<0.1	<0.1	<0.1	<0.1	<0.1
TDS (mg/L)	1249		8862		17485	
Total (ppm)		1250		8872		17505

2.4 Density and Viscosity Measurements

Fluid density significantly effects the IFT measurements, therefore, it should be measured with high accuracy (Moeini et al., 2014). All fluid densities were measured using the high-pressure-high-temperature vibrating tube densitometer (Anton-Paar, Australia) presented in figure 2.1. Fluid densities at ambient conditions were measured using the Pycnometer. Canon-Fenske (presented in figure 2.2.b) was used to measure the viscosity of the prepared brines.

Figure 2.1: HPHT vibrating tube densitometer

(a)
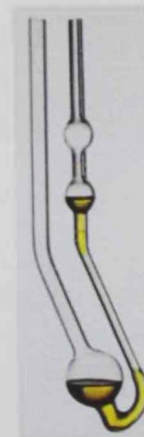
(b)

Figure 2.2: a) Pycnometer b) Canon-Fenske

2.5 Core Samples

The initial plan of the project was to conduct all the tests on rocks and fluids of the Asab formation. Unfortunately, Asab carbonate cores plugs were not available, so the experiments had to be carried out on carbonate core plugs from a nearby formation that could best resembled the Asab formation in terms of physical and chemical properties.

Eleven nearly identical equate pieces of approximately 1.5" diameter grey colored limestone cores were used in this study. All core plugs showed to be completely limestone ($CaCO_3$) as they strongly reacted with HCl acid. Hand lens examinations showed a high porosity and light colored roughly spherical grains partly cemented by sparry calcite.

2.5.1 Thin Section Examination

A thin section of cores number 2 and 13 was prepared as presented in figure 2.3.
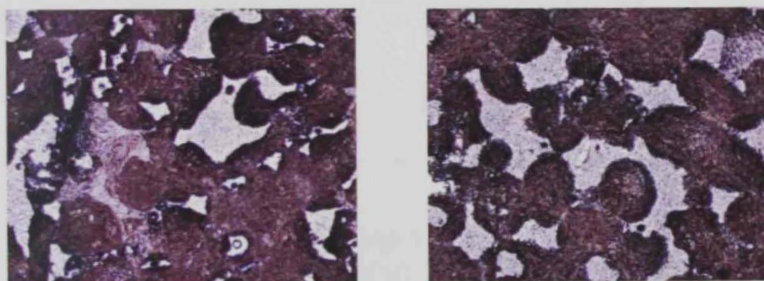
Figure 2.3: Thin section images of cores number 2 and 13

The dominant framework grains are millimeter scale, roughly circular/elliptical and less regular but rounded particles of ultrafine grained carbonate mud, commonly hosting numerous microfossils, including benthonic foraminifera and small fragments of pelecypods and echinoids. Algal particles may also be present. Large sparry calcite crystals occupy pore spaces and oil stains. The percentage of pore space is difficult to

determine due to plucking of grains. The large size of calcite crystals suggests that pore spaces are well-connected, indicating high permeability. The rounded framework are filled with microfossils and did not show any concentric radial structure. This argues against them being identified as oolites or peloids. The particles are probably best described as fossiliferous intraclasts. The rock may be considered as a grainstone and as an intrasparite. Environment in which this rock could form is a tidal flat with fossiliferous muds later disrupted at high tide. The particles would then be rounded and sorted and redeposited in tidal channels. More information on the stratigraphic thickness of the unit and its extent would be needed to test this hypothesis.

2.5.2 Physical Properties of the Core Samples

All eleven carbonate core samples of Um Al Sheif formation were selected and prepared for the study (refer to Appendix D for core preparation procedures). The cores were then screened based on their density, porosity and permeability to air measured using Vinci PoroPerm instrument as described in Appendix E. The basic physical properties used for screening purposes are presented in table 2.6.

Table 2.6: Physical properties of Um Al Shaif core plugs

Sample Number	Sample Name	Diameter (mm)	Length (mm)	Grain Density (g/cc)	Porosity by Air	K by Air (mD)	Selected? Yes/No
1	UmSheif_1	38.11	51.58	2.72	0.18	26.3	no
2	UmSheif_2	38.125	50.7	2.71	0.14	17.8	yes
3	UmSheif_3	38.125	51.67	2.71	0.15	10.4	no
4	UmSheif_5	38.125	52.1	2.73	0.18	13.9	yes
5	UmSheif_8	38.125	51.76	2.71	0.19	15.8	yes
6	UmSheif_371	38.125	50.09	2.72	0.18	16	yes
7	UmSheif_9	38.115	50.7	2.71	0.16	15.2	yes
8	UmSheif_10	37.76	51.447	2.781	0.18	0.045	no
9	UmSheif_13	38.125	50.37	2.71	0.15	14.3	yes
10	UmSheif_16	38.14	50.9	2.71	0.15	23.4	yes
11	UmSheif_24	38.13	50.91	2.71	0.13	8.8	yes

Out of the eleven core plugs available, eight cores were selected for this study. The selection was done mainly based on the porosity and permeability. Samples number 2, 5, 8, 371, 9 and 13 were used for sequential flooding experiments, and core samples number 5 (cleaned and saturated after LSWF), 16 and 24 were selected for spontaneous drainage studies in AMOTT tubes.

All cores plugs were then oil flooded to irreducible water saturation, S_{wirr} and aged for a period of 40 days at 80 °C before core flooding or spontaneous imbibition studies ("Fundamentals of Wettability (Oilfield Review) | Schlumberger." n.d.).

2.6 Interfacial Tension Measurements

Interfacial tensions between oil and the various smart water flooding candidates was measured by pendant drop technique using a Teclis Tracker shown in figure 2.6. The technique consists of partially releasing a drop of oil with a precisely controlled volume into container filled with water. The IFT values were first measured at ambient conditions. Pressure has a negligible effect on the IFT values while the increase in temperature of the fluids could significantly reduce IFT as the solubility of the sulfate ion increase in the water (Strand et al., 2006). Figure 2.4 shows the solubility of $CaSO_4$ in seawater as a function of temperature. The procedures followed for measurement of IFT are included in appendix F.
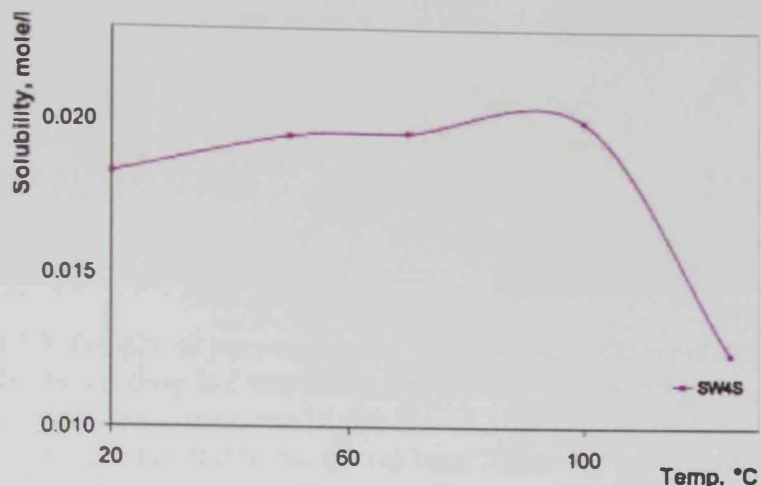
Figure 2.4: Solubility of CaSO₄ in seawater at different temperatures (Strand et al., 2006)

2.7 Contact Angle Measurements

Contact angle measurement is one of the main means to observe the wettability alterations (Yousef et al., 2010). Contact angle values were measured at a maximum temperature of 90 °C and the required pressure to prevent the evaporation of the water (approximately 250 psia). Contact angle is easiest to be measured when the surface is smooth, as surface rigidity confound the visualization of contact angle("Fundamentals of Wettability (Oilfield Review) | Schlumberger," n.d.). Trim-ends were prepared from Asab core sample with low porosity and permeability and aged in oil for 4 weeks at ambient conditions to resemble the oil wet conditions of a carbonate reservoir. Trim-ends were then placed in the corresponding smart water candidate and the contact angle was automatically measured using Teclic-Tracker (shown in figure 2.6) for 72 hours. This technique could best represent the reservoir conditions as it monitors the spontaneous "imbibition" of the brine into the trim-end fully saturated with oil.

$$\theta \sim 0° \qquad \gamma_{so} = \gamma_{sw} + \gamma_{ow} \cos \theta \qquad \theta \sim 180°$$
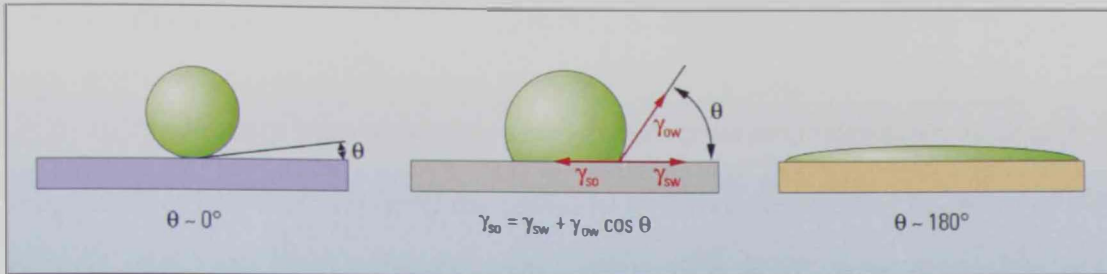
Figure 2.5: Graphical presentation of contact angle. On a perfectly water-wet surface (left) the oil drop is completely surrounded with water giving a ϴ of zero. In a perfectly oil-wet conditions (right) the oil sticks to the rock making a ϴ of zero. In intermediate-wet conditions, the oil bead forms but with an angle that comes from the balancing forces of surface-oil and surface-water ("Fundamentals of Wettability (Oilfield Review) | Schlumberger," n.d.)

The procedures followed for contact angle measurements are included in Appendix F.

Figure 2.6: Teclic-Tracker used for IFT and contact angle measurements

2.8 Core Flooding

Core flooding was intended to assess potential waters under dynamic condition and compare their recovery with the recovery factor achieved from injection of IW. Flooding experiments were designed to evaluate the effect of dilution and sulfate spiking on the oil recovery. A series of six core flooding experiments were conducted for this purpose. Every single core was flooded with specific set of brines sequentially, to eliminate the effect of variation in the rock's petrophysical properties. Table 2.7 shows the order of the injected brines for every core flooding experiment.

Table 2.7: Core flooding experiments

Flooding #	Core #	Order of Brines Injected		
		First	Second	Third
1	UmSheif_5	SW	SWx2SO$_4$	SWx6SO$_4$
2	UmSheif_8	SW/10	SW/10x2SO$_4$	SW/10x6SO$_4$
3	UmSheif_371	SW/50	SW/50x2SO$_4$	SW/50x6SO$_4$
4	UmSheif_2	SW	SWx2SO$_4$	SWx6SO$_4$
5	UmSheif_13	SW	SW/10	SW/50
6	UmSheif_9	IW	SW/10	-

Low Salinity water flooding experiments number 1 to 3 were conducted to evaluate the effect of sulfate spiking on oil recovery. The forth flooding experiments was done to quality check the results of core LSWF number 1. The results of the first four core flooding experiments have driven us toward evaluating the effect of dilution on oil recovery in the fifth LSWF. The sixth flooding experiment was done to conclude the work and report the value of incremental oil recovery that can be obtained using the optimum smart water. All effluents were then analyzed for ionic composition, pH, resistivity, turbidity and total suspended solids (TSS).

Core flooding equipment mainly consists of three major parts: Core holder, heating tape and the injection pump. Figure 2.7 shows the process flow diagram (PFD) of the LSWF experiment.
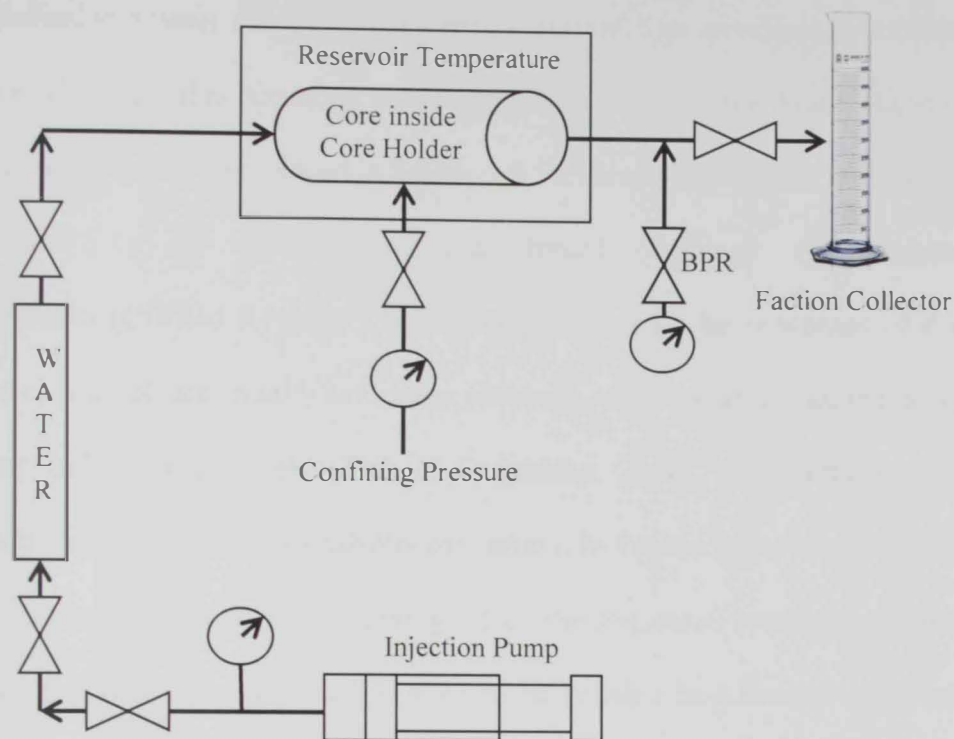
Figure 2.7: Process flow diagram for LSWF experiments

All the tests were conducted under an overburden pressure of 800 psia applied using the hydraulic pump. Fluid displacement was achieved by operating the syringe pump at a constant rate of 2 cc/min. To regulate the flow and avoid extra pressure build-up after heating the system, a back pressure regulator (BPR) was installed to control the outlet pressure at 150 psi (Alotaibi, Azmy, & Nasr-El-Din, 2010). The detailed procedures of core flooding experiments are included in Appendix H.

2.9 Spontaneous Drainage Studies – Amott

The Amott-Harvey method is commonly used to measure the reservoir wetting phase (Boneau & Clampitt, 1977). A sample at irreducible water saturation, S_{wirr} is immersed in a water-filled tube for a period of time. The spontaneous imbibition takes place when the oil is displaced with surrounding water. In the Amott Harvey method, the core sample is then placed in a flow cell for forced imbibition. The process is then followed by a spontaneous and forced drainage ("Fundamentals of Wettability (Oilfield Review) | Schlumberger," n.d.). The outcomes of the Amott-Harvey method are usually saturation indices I_w and I_o that are saturation change of water and oil respectively (Tiab & Donaldson, 2016). The method is more of a quantitative approach of wettability evaluation. In this study, an Amott tube is utilized for another set of experiments during which the sequential spontaneous imbibition is only monitored. The approach proved to be reliable in quantitatively studying the potential of different waters in enhancing the oil recovery (Strand et al., 2006). All spontaneous imbibition tests were conducted at 90 °C to make sure that the solubility of sulfate in seawater is maximized (RezaeiDoust et. al. 2009; Strand et al., 2006). The Amott tubes used for HTHP conditions were provided with a back pressure valve that could provide the necessary pressure to prevent the boiling of the fluids at high temperature conditions. Figure 2.8 shows the HTHP Amott cells used for this study.

Spontaneous Imbibition   Spontaneous Drainage

Figure 2.8: High temperature Amott Cells (Vinci Technologies, France)

The 40 day aged core samples number 5, 16 and 24 were each placed in one spontaneous imbibition cell. All three Amott cells were used to study exclusively the effect of dilution on oil recovery (brine category number 5). As spontaneous imbibition tests were conducted at high temperature conditions, it was important to minimize the recovery due thermal expansion of the oil (Romanuka et al., 2012). Therefore, all the components used in the spontaneous imbibition (the oil saturated core sample and Amott cell) were heated at the test temperature prior to conducting the experiment. The Amott cell containing the saturated core sample was placed into an air-circulating oven and heated up to 90 °C while the pressure of cell was maintained at 30 psia at all times (to avoid boiling). The spontaneous imbibition tests were first conducted with injection water (IW) and kept until no more oil was produced. The brines were then replaced by the brines of category 5 sequentially and kept under high temperature conditions until no extra oil production could be observed. Table 2.8 shows the order of the brines used.

Table 2.8: Order of brines used in high temperature spontaneous imbibition

Brine Order	*Duration (days)*	Brine Name
1	1 to 10	IW
2	10 to 20	SW
3	20 to 30	SW/10
4	30 to 40	SW/50

Monitoring and measuring the oil produced by capillary imbibition began as soon as the assembly of the Amott set-up was complete. The recovered oil was then presented as a percentage of OIIP as a function of time. Detailed procedures of conduction spontaneous imbibition tests are included in Appendix G. Figure 2.8 schematically describes the spontaneous capillary imbibition of oil.
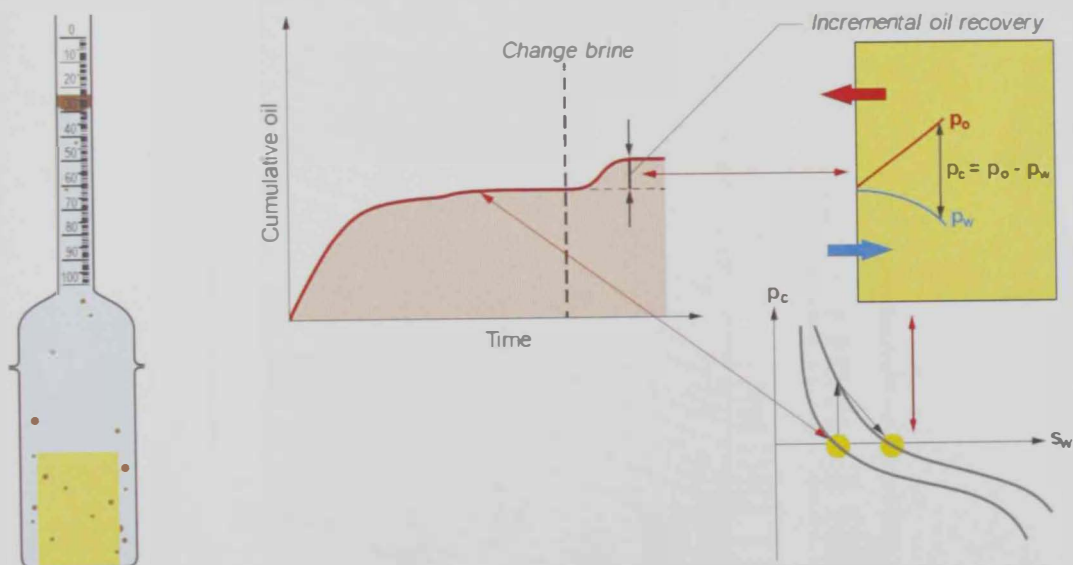
Figure 2.9: Graphical presentation of spontaneous imbibition. a) Schematic description of the core plug at S_{wirr} at the Amott tube. The produced oil (with a density lower than water) is then collected at the top and measured accordingly. b) A schematic representation of the sequential Amott Imbibition test (Romanuka et al., 2012).

Chapter 3: Results and Discussions

3.1 Brine Properties

Brines were prepared using the procedures described in Appendix A to Appendix C. The viscosities and densities of the prepared brines were then measured at ambient conditions using a Pycnometer and cannon flask. The pH values were measured using a digital pH meter right after the brine preparation.

A simple and straightforward measure of salinity of a conductive fluid would be the resistivity (Tiab & Donaldson, 2016). The resistivity at a specific temperature can be simply correlated with the equivalent NaCl concentration in the fluid using figure 3.1.
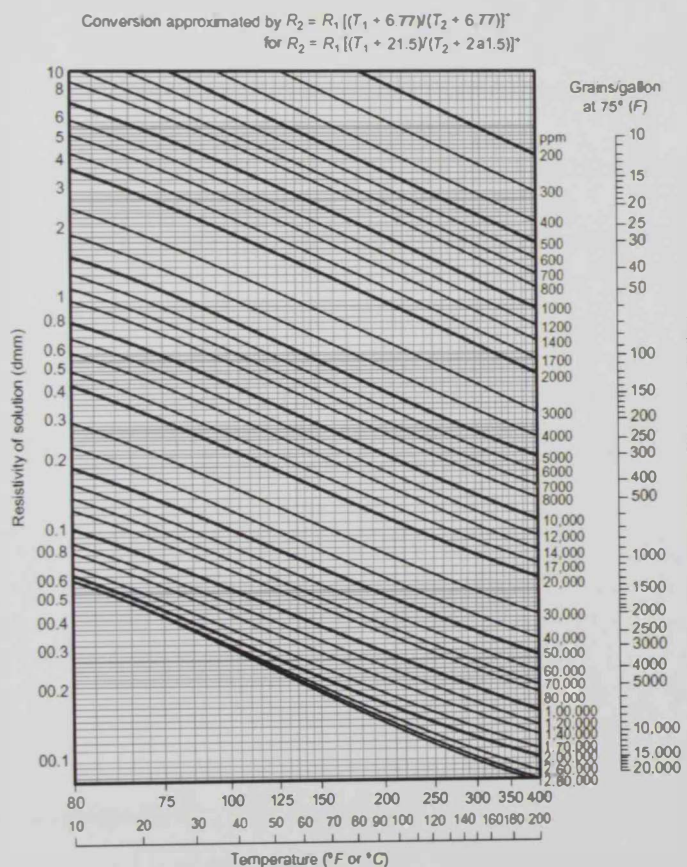
Figure 3.1: Water resistivity as a function of NaCl concentration and temperature (Tiab & Donaldson, 2016)

The resistivity values of the prepared brines were measured using digital brine resistometer at room temperature of 23 °C. The results are presented in table 3.1.

Table 3.1: Measured properties of brines

Brine	Salinity ppm	Density g/ml	Viscosity cp	pH	Resistivity Ω m
FW	157662	1.1034	1.3483	7.21	52.0
IW	256551	1.1639	1.75	6.60	34.5
SW	62522	1.0398	1.1901	7.32	76.6
SW x2 SO4	65990	1.0420	1.2049	7.33	78.9
SW x6 SO4	72927	1.0464	1.2566	7.37	77.3
SW/10	6252	1.0005	1.0724	7.25	621.7
SW/10 x2 SO4	8872	1.0027	1.0836	7.29	511.7
SW/10 x6 SO4	17505	1.0075	1.0987	7.35	389.1
SW/50	1250	1.0001	1.0315	6.70	2755.1
SW/50 x2 SO4	4719	1.0005	1.0702	6.70	1285.8
SW/50 x6 SO4	11655	1.0039	1.0894	6.75	508.5
DI water	0	1.0000	1.01	6.50	-

Increasing the ionic concentration and TDS of brines resulted in an increase in density and viscosity. The addition of sulfate as a polyatomic anionic surfactant had minor effects on increasing the viscosity. The results of density and viscosity are presented in figure 3.2.
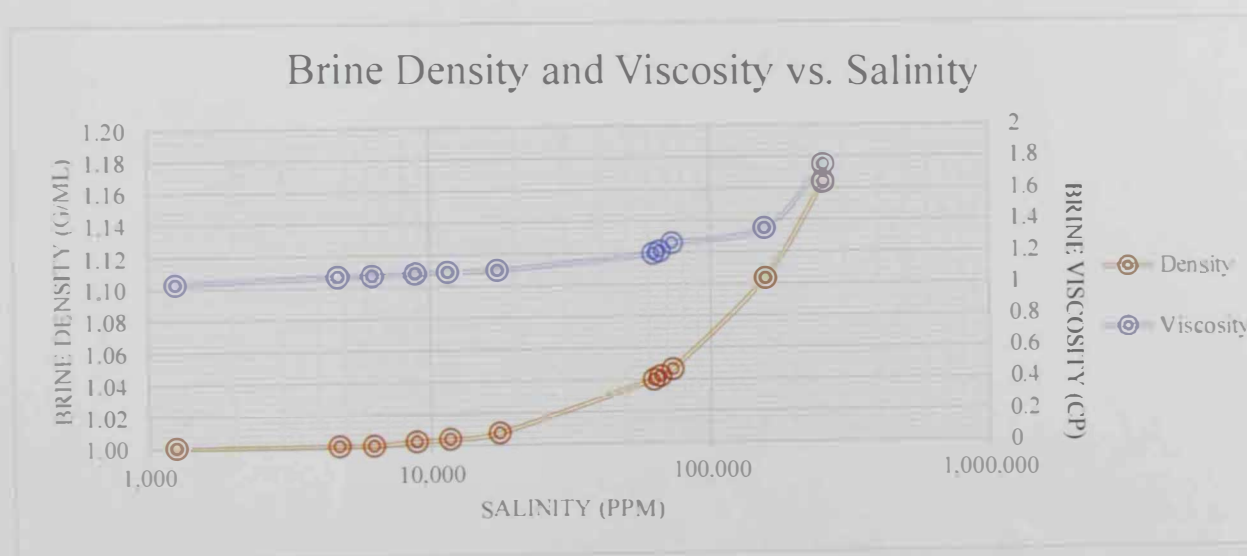
Figure 3.2: Brine density and viscosity vs. brine salinity in ppm

The pH values indicated that all the brine used in this study had been initially neutral. There was no trend that could be related with salinity or concentration of any specific ion. The slight reduction of the pH by dilution is explained by the lower pH value of DI water used for dilution. Figure 3.3 represents the pH variation for different brines.
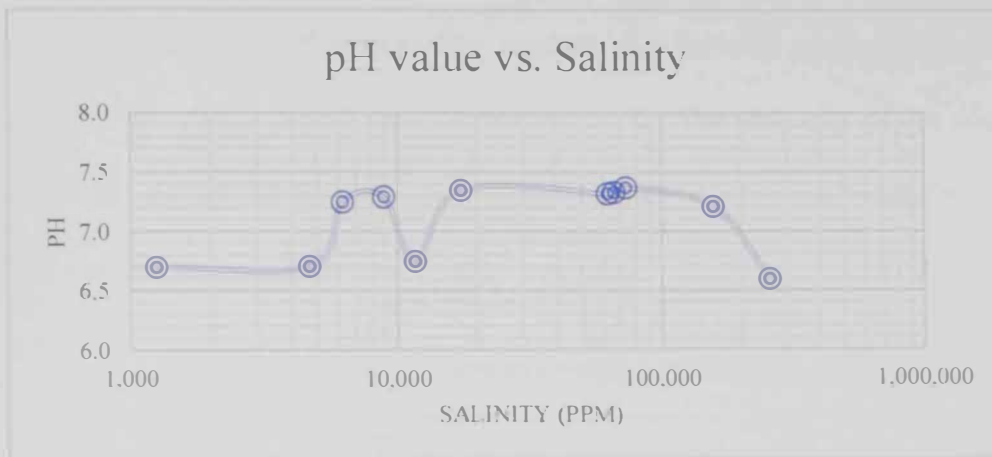
Figure 3.3: Values of pH vs. brine salinity in ppm

There was an inverse relationship between resistivity and total salinity of the brine. Figure 3.4 shows the resistivity results vs. total salinity (ppm) at a room temperature of 23 °C.
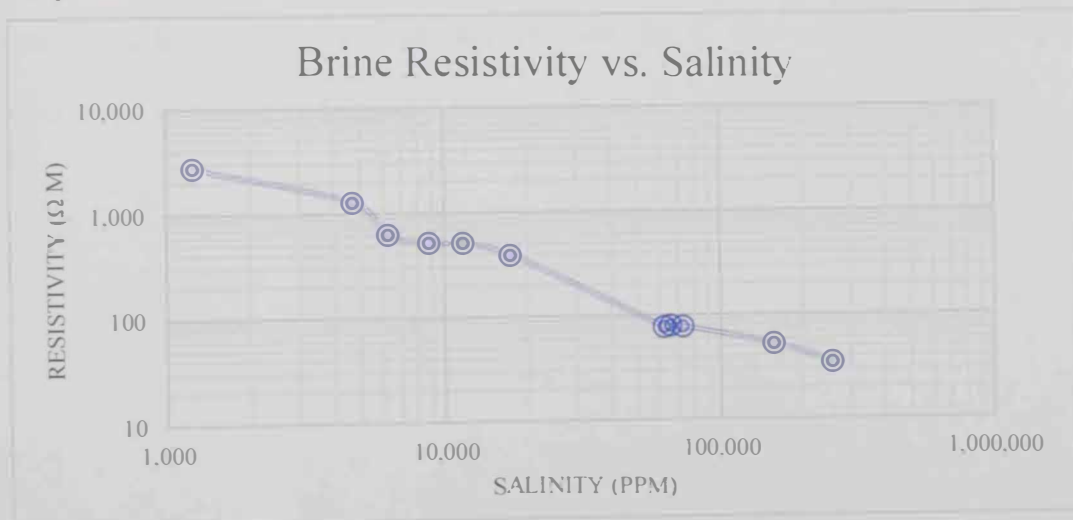
Figure 3.4: Brine resistivity vs. salinity in ppm

3.2 Oil Properties

The measured properties of the dead oil are subdivided into physical and chemical properties.

3.2.1 Physical Properties

Density and API values of the dead oil were measured using both a hydrometer and an Anton Paar digital densitometer at 20 °C. The viscosity of the dead oil was measured at reservoir temperature and various pressures using a Vinci (France) rolling ball viscometer.

Table 3.2: Physical properties of crude oil

Property	Unit	Value
Gravity at 20 °C	API	39.48
Density at 20 °C	g/cc	0.8276
Viscosity at 20 °C & 14.7 psia	mPa.s-cP	2.927
Viscosity at 123°C (255°F) & 3100 psia (P_{res})	mPa.s-cP	1.8593

Table 3.2 shows a summary of the measured physical properties of the crude oil. The results of the rolling ball viscometer at a reservoir temperature of 255 °F indicate that increasing the pressure will slightly increase the oil viscosity. Dynamic viscosity results are presented in figure 3.5.

Dynamic Viscosity vs. Pessure
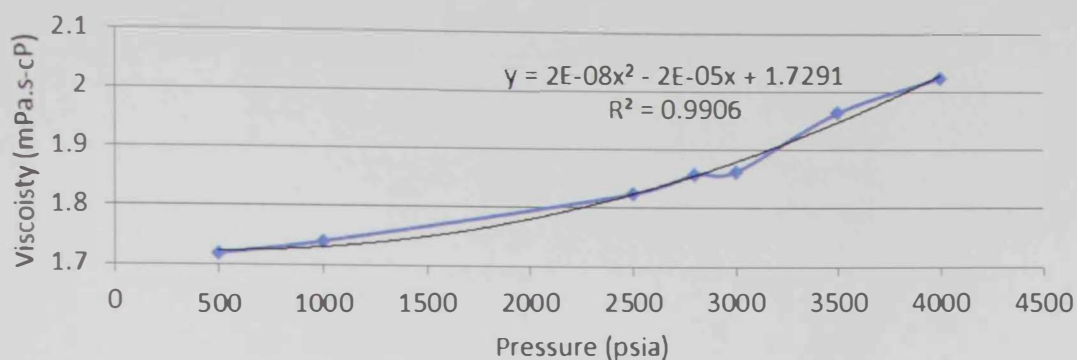
Figure 3.5: Dynamic viscosity of oil (at 255 °F) vs. pressure

3.2.2 Chemical Properties

The acidity of oil is very low, thus, a very diluted solution of KOH had to be used for titration and AN measurement. The value of the acid number was 0.07 mg KOH/g. The low acid number value represents the neutral-wet state of the rock. To have a more complete image of the oil chemical properties, an available gas chromatography (CG) analysis was also conducted. Results of GC analysis are presented in table 3.3.

Table 3.3: Gas chromatography results of the dead oil sample

Number	Substance	Mole Fraction
1	C9	0.50019
2	C10	0.00022
3	C11	0.00039
4	C12	0.03773
5	C13	0.04466
6	C14	0.00810
7	C15	0.09362
8	C16	0.01655
9	C17	0.01747
10	PRISTANE	0.07574
11	C18	0.01175
12	PHYTANE	0.07414
13	C19	0.01318
14	C20	0.00740
15	C21	0.01219
16	C22	0.01330
17	C23	0.01425
18	C24	0.01227
19	C25	0.01062
20	C26	0.00852
21	C27	0.00712
22	C28	0.00554
23	C29	0.00288
24	C30	0.00397
25	C31	0.00330
26	C32	0.00284
27	C33	0.00019
28	C34	0.00025
29	C35	0.00083
30	C36	0.00053
31	C37	0.00021
32	C38	0.00004
	Totals:	1

Light organic components make up the majority of the crude oil mixture. This explains having a light oil with an API gravity of 39.5.

3.3 Interfacial Tension and Contact Angle Studies

The values of IFT and a contact angle (at 90 °C) for various brines were measured during the early stages of this project and have been presented in MSc thesis of Jassim Abubacker (Jassim Abubacker Ponnambathayil, 2016). Table 3.4 presents a summary of these findings.

Table 3.4: Results of IFT and contact angle studies at HPHT conditions

Brine	$[SO_4^{2-}]$ (mg/L)	IFT (dyne/cm)	Contact Angle (degree)
SW	3949	9.503	113
SW x 2SO4	5719	10	138
SW x 6SO4	9259	8.343	162
SW/10	395	11.741	131
SW/10 x 2SO4	2165	11.145	123
SW/10 x 6SO4	5705	10.351	142
SW/50	79	13.86	114
SW/50 x 2SO4	1849	13.406	147
SW/50 x 6SO4	5389	12.992	148

The results of the IFT measurements indicated that lower IFT values could be obtained with higher concentrations of sulfate ions. No significant trend could be found between the contact angle measurements and the dilution/spiking. The lowest contact angle could be obtained with seawater. Based on the static studies of IFT and contact angle, seawater with no spike in sulfate content was selected as the potential smart water. Further tests (static and dynamic) were conducted to verify this this conclusion.

3.4 Oil flooding experiments

All the selected UmAlsheif core plugs were flooded with water to measure their absolute permeability to water (column 5) and the brine saturated pore volume (column 3) using the procedure described in Appendix E. The core plugs were then

flooded with Asab Crude oil (following the procedure described in appendix H) until no water is produced. The cumulative volume of water produced (column 6), is then used to calculate the initial water (column 7) and oil (column 8) saturations. The results presented in column 2 and 4 are the porosity and permeability measurements obtained initially using PoroPerm (vinci) for core screening purposes. Results of the oil flooding experiments are presented in table 3.5.

Table 3.5: Results of oil flooding experiments

	[1]	[2]	[3]	[4]	[5]	[6]	[7]	[8]
Sample Number	Sample Name	Porosity by Air	Porosity by Water	K by Air (mD)	K by Water (mD)	Produced Water (cc)	S_{wi} (%)	S_{oi} (%)
1	UmSheif_2	0.14	0.12	17.8	10.3	4.20	38.0	62.0
2	UmSheif_5	0.18	0.14	13.9	11.6	5.35	38.1	61.9
3	UmSheif_8	0.19	0.16	15.8	12.2	5.85	41.2	58.8
4	UmSheif_371	0.18	0.15	16	11.2	5.60	33.3	66.7
5	UmSheif_9	0.16	0.14	15.2	10.8	4.60	39.4	60.6
6	UmSheif_13	0.15	0.14	14.3	11.2	5.50	35.0	65.0
7	UmSheif_16	0.15	0.11	23.4	20.6	3.50	59.9	40.1
8	UmSheif_24	0.13	0.11	8.8	7.6	4.00	48.8	51.2

The initial water saturation in the core plugs varies between 33 to 40%. The core were then aged in Asab oil for 40 days at a high temperature of 80 °C. To evaluate any wettability alteration due to aging (toward a more oil wet state), the cores were flooded again with oil and the incremental volume of produced water was measured. No extra water was produced after aging illustrating that no significant wettability alteration was observed.

3.5 Low Salinity Water Flooding Experiments

For every core flooding experiment, values of the oil recovery factor for of different brines is reported as a function of pore volume injected. The oil Recovery

factor was calculated by dividing the volume of the produced oil by the volume of oil initially in place.

3.5.1 LSWF Number 1 (Brine Category 2)

In the first core flooding experiment, core number 5 with a S_{wi} of 38.1 % was flooded with sea water at different sulfate concentrations. Table 3.6 shows the results of the first core flooding experiment.

Table 3.6: Core flooding results for LSWF number 1

Injected Water	Tube #	W_i (cc)	V_{oil} Produced		W_i (PV)	RF (%)
			Per tube	Cumulative		
SW	0	0	0	0	0	0.00
	1.1	2.8	1.4	1.4	0.3	26.17
	1.2	1.67	0.42	1.82	0.5	34.02
	1.3	2	0	1.82	0.8	34.02
	1.4	2	0	1.82	1.0	34.02
	1.5	2	0.12	1.94	1.2	36.26
	1.6	2	0	1.94	1.5	36.26
	1.7	4.65	0.05	1.99	2.0	37.20
	1.8	4.3	0.05	2.04	2.5	38.13
	1.9	4.7	0.1	2.14	3.1	40.00
	1.10	5.3	0.02	2.16	3.7	40.37
	1.11	13	0.01	2.17	5.2	40.56
	1.12	14.6	0.01	2.18	6.9	**40.75**
SW x2SO4	2.1	12	0	2.18	8.3	40.75
	2.2	13	0	2.18	9.8	40.75
	2.3	52	0	2.18	15.9	**40.75**
SW x6SO4	3.1	12.2	0	2.18	17.3	40.75
	3.2	14	0	2.18	19.0	40.75
	3.3	51	0	2.18	24.9	**40.75**

Figure 3.6 shows the oil recovery factor for various values of pore volume injected.
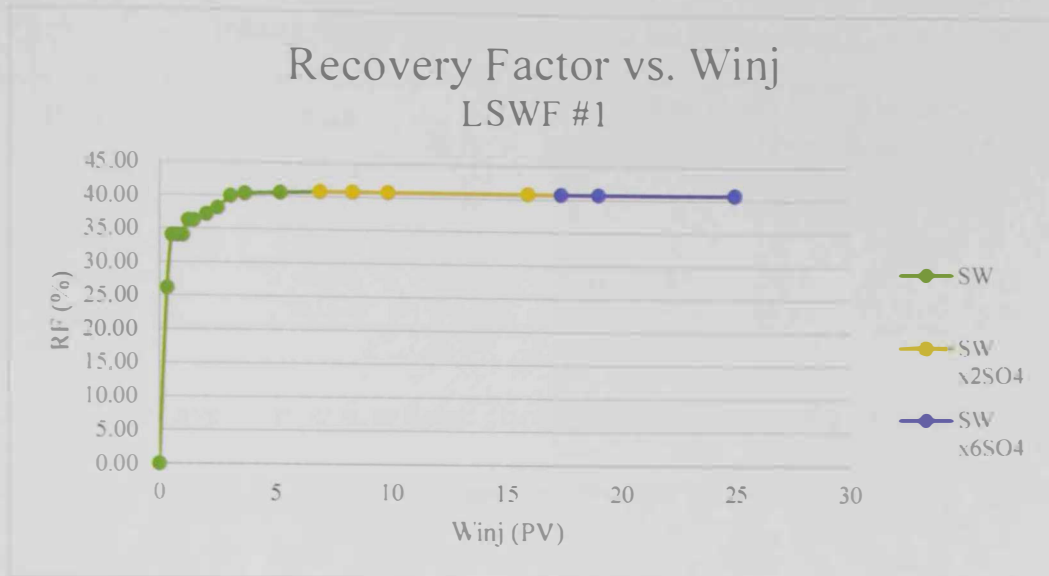
Figure 3.6: Recovery factor versus pore volume injected for LSWF number 1

The sulfate spiking showed no effect on increasing oil recovery. No significant change in the endpoint effective permeability to water was observed by increasing the sulfate concentration. The values of end point effective permeability for each injected brine is presented in figure 3.7.
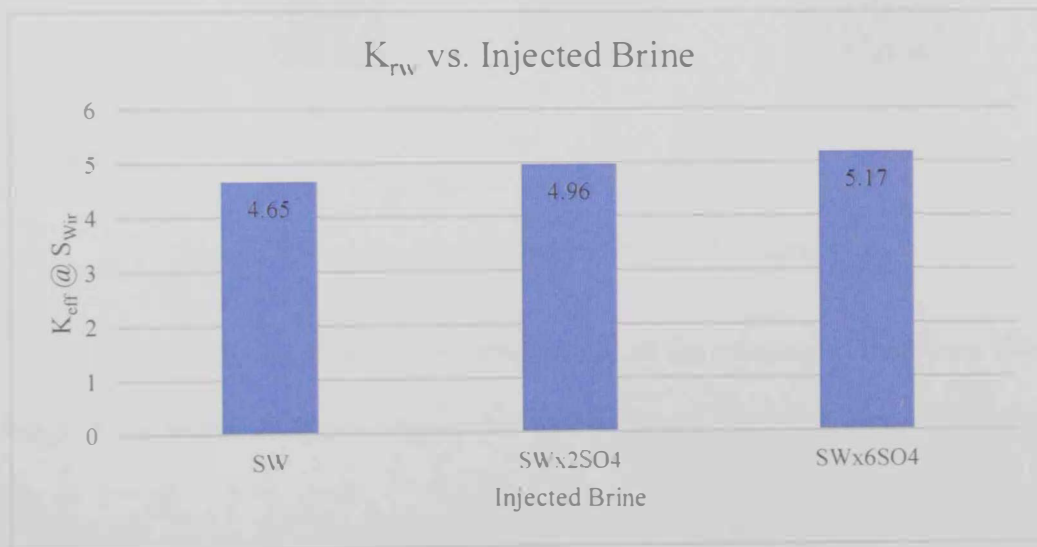
Figure 3.7: End-point effective permeability for LSWF #1

Other important properties that could be used for investigating the recovery mechanism are listed in table 3.7.

Table 3.7: Effluent properties for LSWF number 1

Parameter	Unit	SW		SW x2 SO_4^{2-}		SW x6 SO_4^{2-}	
		Before	After	Before	After	Before	After
pH	log(mol/L)	7.32	7.03	7.33	7.18	7.37	7.24
Turbidity	NTU	0	8	0	7	0	9
Suspended Solids	mg/L	0	4	0	3	0	7
Hardness	mg/L	2851	2876	2851	2916	2851	2822
Resistivity	mΩ-m	76.60	82.90	78.90	80.50	77.30	78.43

There have been no significant alteration in the acidity of the effluents. Figure 3.8 shows the pH values of the injected brines, before and after the flooding experiment.
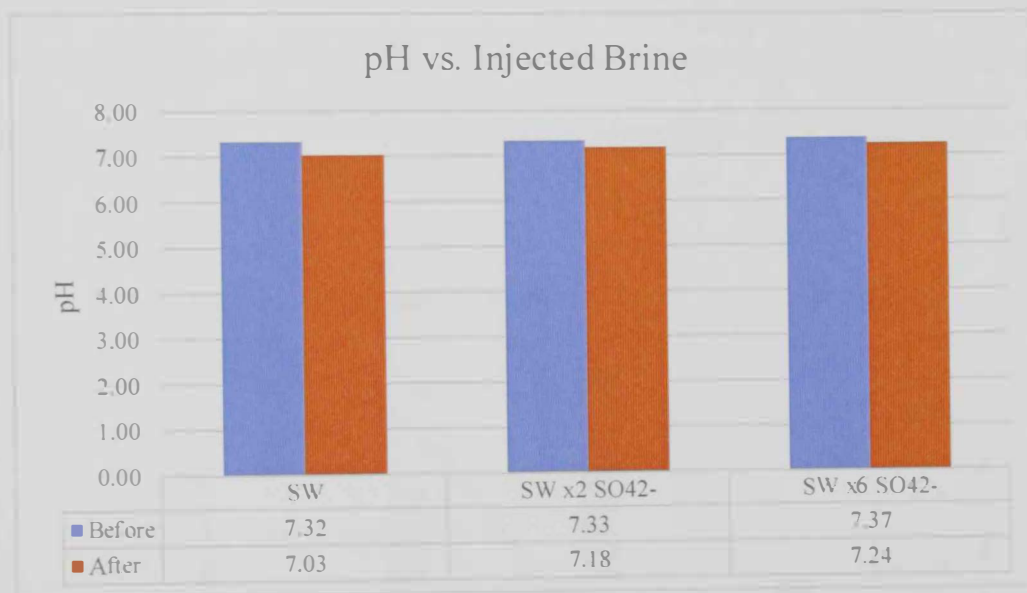
Figure 3.8: pH value of effluents for LSWF number 1

Before conducting the LSWF experiment, all the prepared brines were filtered through three layers of 5 μm filter paper to ensure they have zero turbidity and no

suspended solids. After LSWF, there was a slight increase in turbidity and amount of suspended solids in effluent as presented in figure 3.9
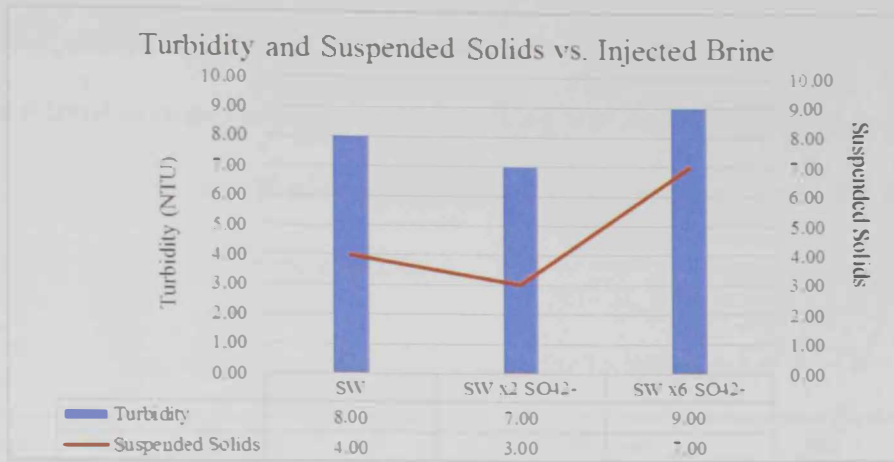
Figure 3.9: Turbidity and Total Suspended Solids for LSWF number 1

The resistivity and water hardness values were measured for all effluents to observe any change in salinity or possible rock dissolution. There have been no significant alteration in the salinity or hardness of the effluents of LSWF number 1.
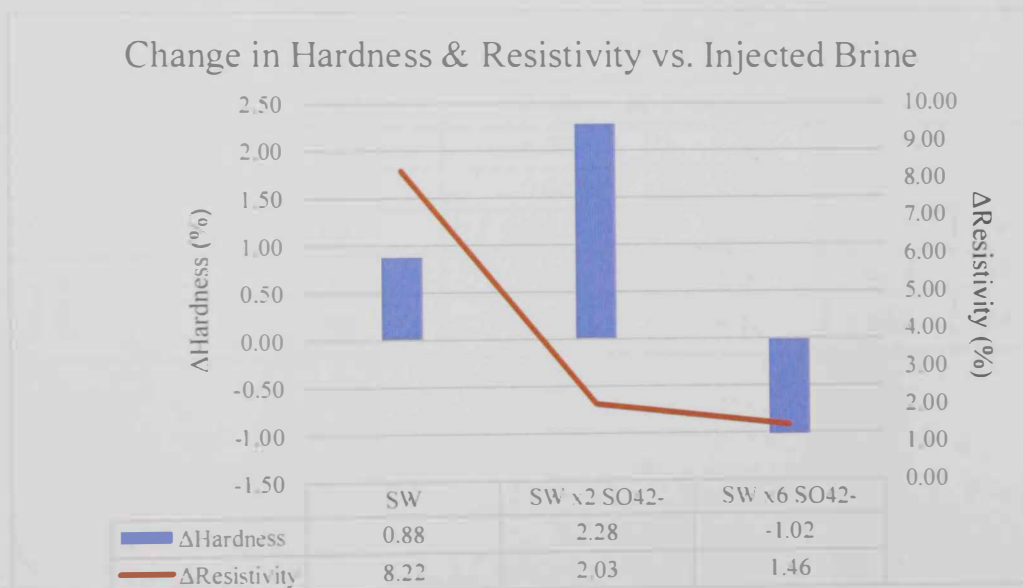
Figure 3.10: Change in Water Hardness and Resistivity for LSWF number 1

3.5.2 LSWF Number 2 (Brine Category 3)

In the second low salinity water flooding experiment, core number 8 with an initial water saturation of 41.2 % and initial oil volume of 5.85 cc, was flooded with 10 times diluted seawater samples. Sulfate spiking was also attempted to evaluate any possible contribution of sulfate in increasing crude oil recovery. Table 3.8 shows the results of the second LSWF experiment.

Table 3.8: Core flooding results for LSWF number 2

Injected Water	Tube #	W_i (cc)	V_{oil} Produced		W_i (PV)	RF (%)
			Per tube	Cumulative		
SW/10	0	0	0.00	0.00	0.0	0.00
	1.1	1.88	0.38	0.38	0.2	6.50
	1.2	0.82	0.82	1.20	0.3	20.51
	1.3	0.8	0.35	1.55	0.4	26.50
	1.4	0.8	0.25	1.80	0.5	30.77
	1.5	1.65	0.20	2.00	0.6	34.19
	1.6	1.5	0.00	2.00	0.8	34.19
	1.7	1.87	0.27	2.27	1.0	38.80
	1.8	8.5	0.30	2.57	1.9	43.93
	1.9	52.5	0.60	3.17	7.4	54.19
	1.10	100.5	0.20	3.37	17.9	57.61
	1.11	100	0.02	3.39	28.4	**57.95**
SW/10 x2SO4	2.1	13.5	0.00	3.39	29.8	57.95
	2.2	13	0.00	3.39	31.1	57.95
	2.3	100	0.01	3.40	41.6	**58.12**
SW/10 x6SO4	3.1	15	0.00	3.40	43.2	58.12
	3.2	50	0.00	3.40	48.4	**58.12**

Figure 3.11 shows the oil recovery factor for various values of pore volume injected.
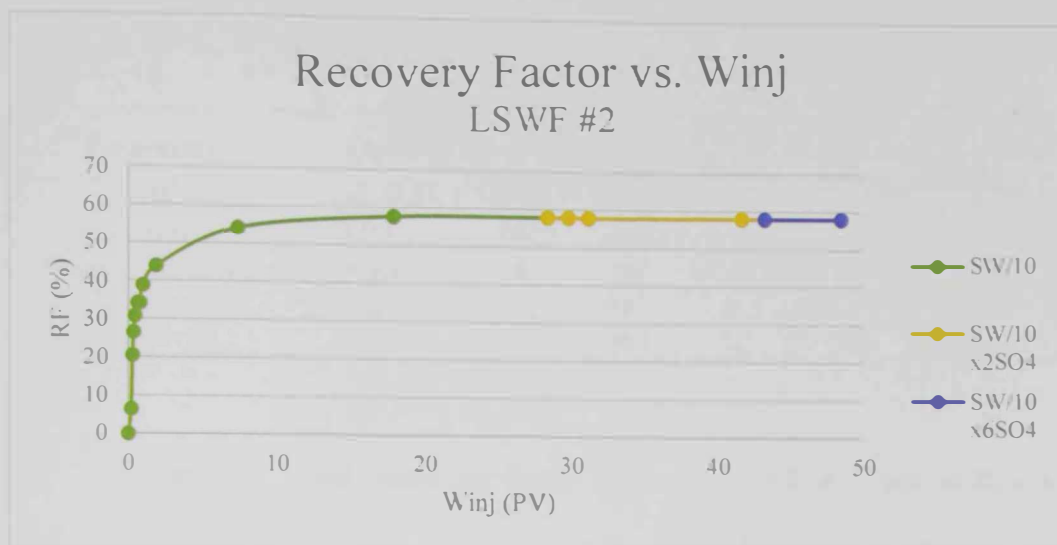
Figure 3.11: Recovery factor versus pore volume injected for LSWF number 2

No significant oil recovery could be observed when the core plug was flooded with 10 times diluted brines with higher sulfate concentrations. Results indicated that a substantial increase in the values of end-point effective permeability to water can be achieved when the core is continuously flooded with diluted brines. The values of end point effective permeability for each injected brine is presented in figure 3.12.
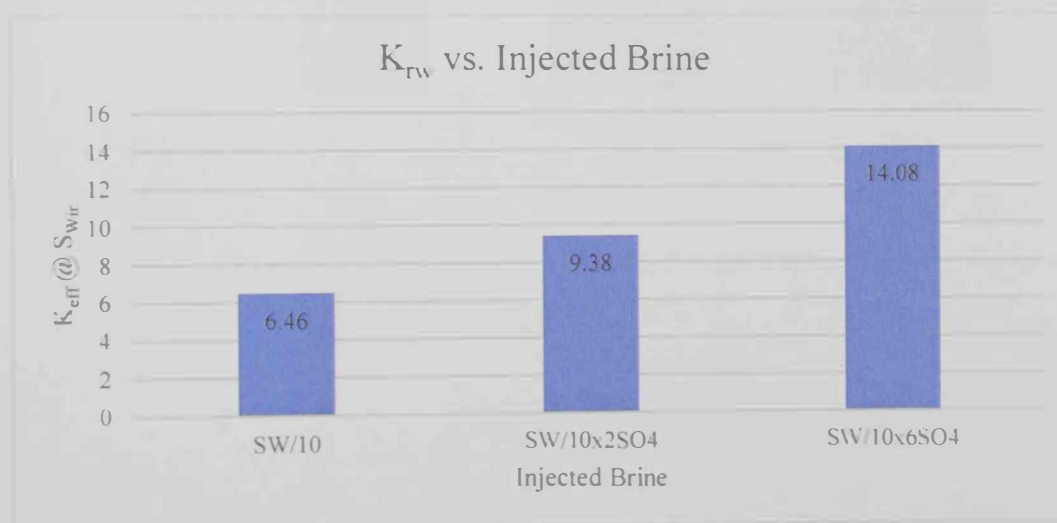
Figure 3.12: End-point effective permeability for LSWF #2

Additional important properties of the effluents that could be used for investigating the mechanism are listed in table 3.9.

Table 3.9: Effluent properties for LSWF number 2

Parameter	Unit	SW/10		SW/10 x2 SO_4^{2-}		SW/10 x6 SO_4^{2-}	
		Before	After	Before	After	Before	After
pH	log(mol/L)	7.25	7.40	7.29	7.43	7.35	7.78
Turbidity	NTU	0	41	0	59	0	38
Suspended Solids	mg/L	0	52	0	64	0	44
Hardness	mg/L	275	982	275	1211	275	873
Resistivity	mΩ-m	622	393	512	336	389	288

No specific trend could be found between LSWF and the acidity of the effluents. Figure 3.13 shows the pH value of the effluents before and after the flooding experiments.
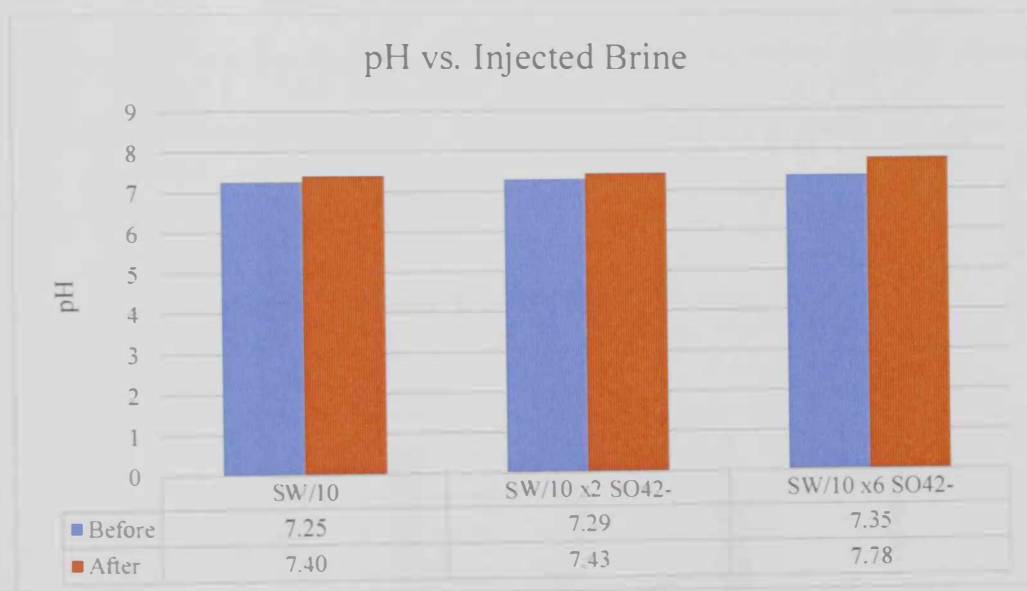
Figure 3.13: pH value of effluents for LSWF number 2

A significant increase in turbidity and the amount of total dissolved solids was observed when the core plug was flooded with 10-times-diluted samples of seawater. The results are presented in figure 3.14.

Figure 3.14: Turbidity and Total Suspended Solids for LSWF number 2

Water turbidity and suspended solids could present any possible cement/matrix dissolution. The hypothesis was verified by measuring the values of brine resistivity to observe the increase in salinity) and water hardness (to measure the increase in calcium) as presented in figure 3.15.
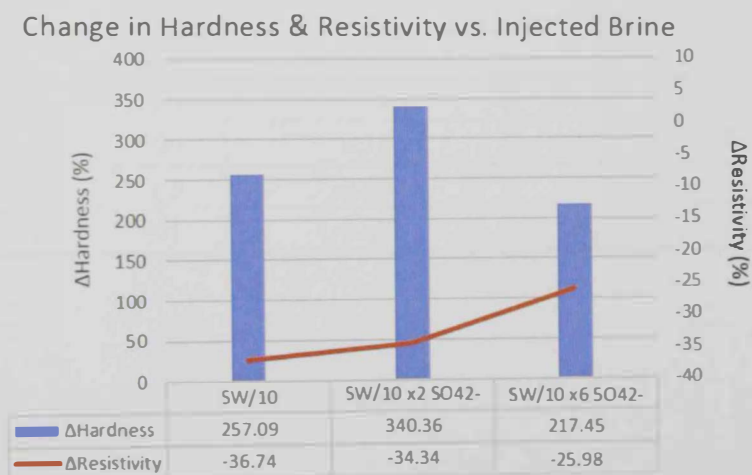
Figure 3.15: Change in Water Hardness and Resistivity for LSWF number 2

The significant increase in both water hardness (reflecting the concentration of calcium and magnesium ions) and water salinity (the reduction in resistivity) have been resulted by rock dissolution.

3.5.3 LSWF Number 3 (Brine Category 4)

To investigate the effect of sulfate in highly diluted brines, core number 371 was flooded using 50-times-diluted seawater at different sulfate concentrations. Table 3.10 shows the results of the third LSWF experiment.

Table 3.10: Core flooding results for LSWF number 3

Injected Water	Tube #	W_i (cc)	V_{oil} Produced		W_i (PV)	RF (%)
			Per tube	Cumulative		
SW/50	1	0.9	0.33	0.33	0.1	5.89
	2	1	1.00	1.33	0.2	23.75
	3	0.8	0.70	2.03	0.3	36.25
	4	0.65	0.38	2.41	0.4	42.95
	5	0.75	0.15	2.56	0.5	45.63
	6	0.87	0.15	2.71	0.6	48.30
	7	3.6	0.30	3.01	1.0	53.66
	8	26.8	0.30	3.31	4.1	59.02
	9	51.3	0.60	3.91	10.2	69.73
	10	50.5	0.10	4.01	16.1	**71.52**
SW/50 x2SO4	2.10	12.5	0.10	4.11	17.5	73.30
	2.2	100	0.10	4.21	29.3	**75.09**
SW/50 x6SO4	3.1	11.5	0.00	4.21	30.6	75.09
	3.2	101	0.00	4.21	42.5	**75.09**

Figure 3.16 shows the oil recovery factor for the three different brines versus the pore volume injected.
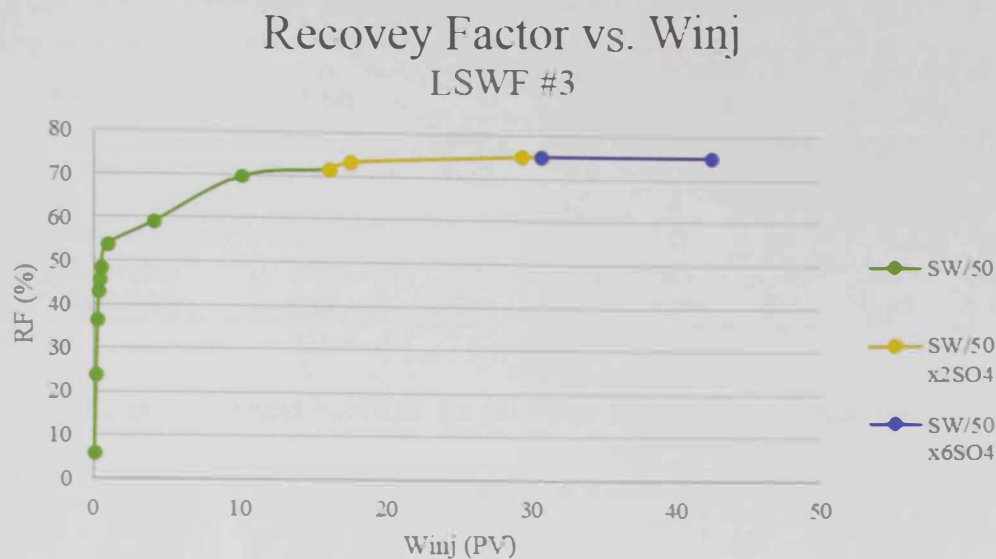
Figure 3.16: Recovery factor versus pore volume injected for LSWF number 3

Increasing the sulfate concentration showed no significant effect on increasing the crude oil recovery. Yet, the results of end-point effective permeability had revalidated the idea of the rock dissolution as presented in figure 3.17.
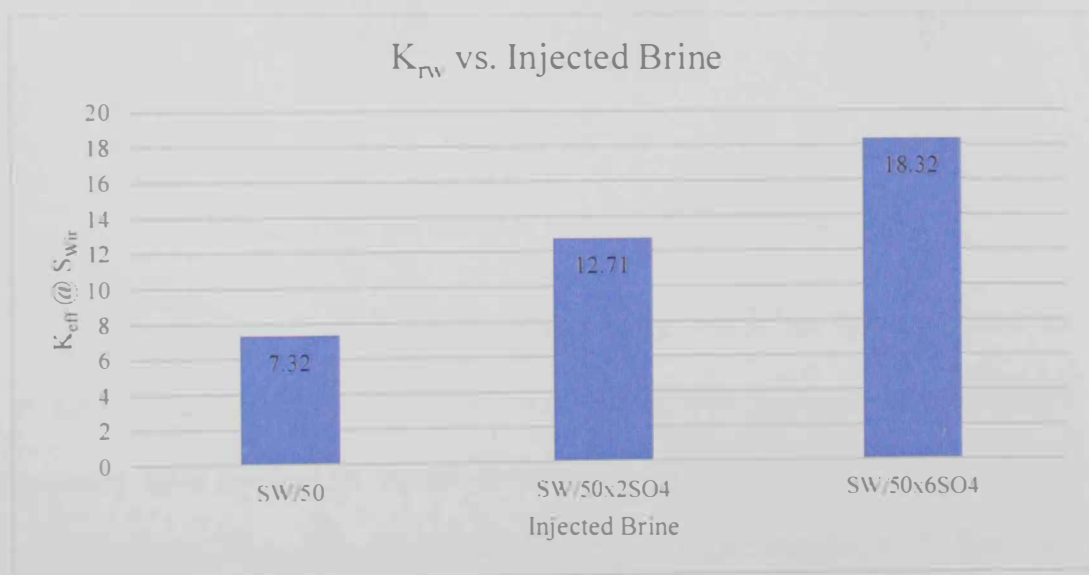
Figure 3.17: End-point effective permeability for LSWF #3

The additional properties of effluents are measured before and after the LSWF experiments and are listed in table 3.11.

Table 3.11: Effluent properties for LSWF number 3

Parameter	Unit	SW/50		SW/50 x2 SO$_4^{2-}$		SW/50 x6 SO$_4^{2-}$	
		Before	After	Before	After	Before	After
pH	log(mol/L)	6.70	7.18	6.70	7.69	6.75	7.38
Turbidity	NTU	0	22	0	31	0	28
Suspended Solids	mg/L	0	30	0	25	0	26
Hardness	mg/L	60	1312	60	1760	60	986
Resistivity	mΩ-m	2755	1358	1286	634	509	231

Likewise, no trend between the pH value and the incremental recovery could be observed for the third LSWF experiment, as shown in figure 3.18.

	SW/50	SW/50 x2 SO42-	SW/50 x6 SO42-
Before	6.70	6.70	6.75
After	7.18	7.69	7.38
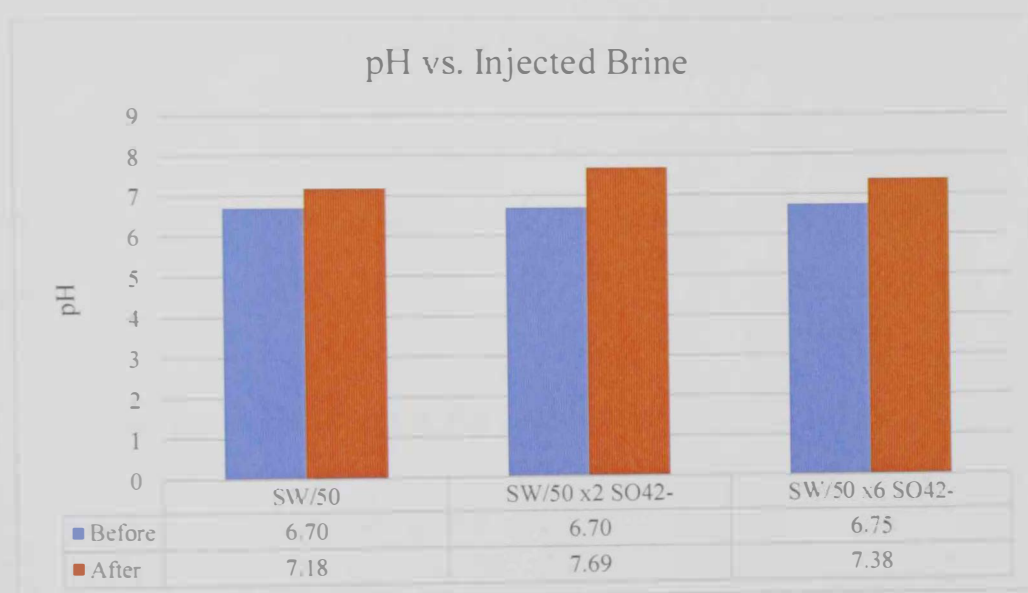
Figure 3.18: pH value of effluents for LSWF number 3

The results of turbidity and the total suspended solids showed a trend similar to LSWF number 2. Flooding the core sample with 50-times-diluted samples of seawater have resulted in similar turbidity but fewer suspended solids. The lower values of suspended solids may be explained by the higher capacity of 50-times-diluted

seawater in dissolving the solid particles. Results of turbidity and TSS are presented in figure 3.19.

Turbidity and Suspended Solids vs. Injected Brine

	SW/50	SW/50 x2 SO42-	SW/50 x6 SO42-
Turbidity	22.00	31.00	28.00
Suspended Solids	30.00	25.00	26.00
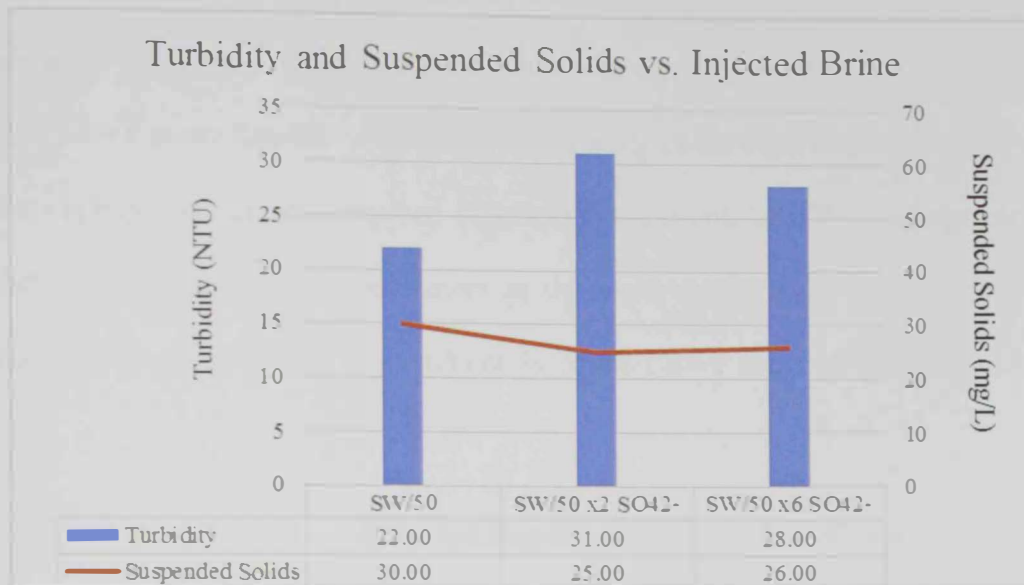
Figure 3.19: Turbidity and Total Suspended Solids for LSWF number 3

The possible rock dissolution have also resulted in a significant increase in water hardness and water salinity (shown by a reduction in resistivity) as illustrated in figure 3.20.

Change in Hardness & Resistivity vs. Injected Brine

	SW/50	SW/50 x2 SO42-	SW/50 x6 SO42-
ΔHardness	2086.67	2833.33	1543.33
ΔResistivity	-50.72	-50.70	-54.61
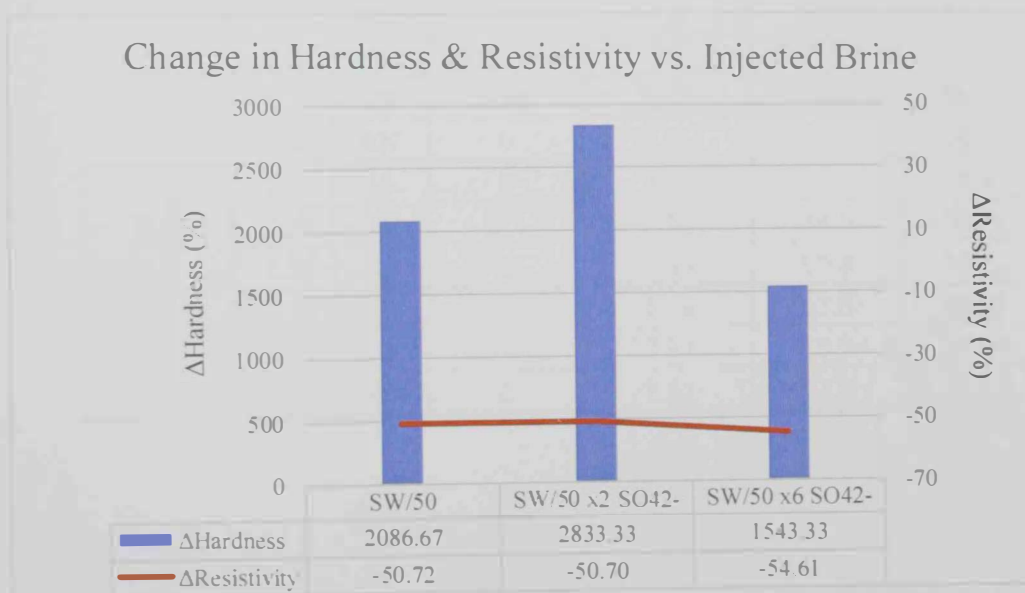
Figure 3.20: Change in Water Hardness and Resistivity for LSWF number 3

3.5.4 LSWF Number 4 (Brine Category 2)

In this experiment, core number 2 was flooded (at a lower injection rate) with seawater at different sulfate concentrations. The results were then compared with the first LSWF to confirm the repeatability and quality of the observations. Similar results but slightly more oil recovery was observed in the fourth LSWF. The recovery factor did not have comparable parameters as the experiments are subjected to different heterogeneity conditions. The results of the fourth LSWF experiment are listed in table 3.12.

Table 3.12: Core flooding results for LSWF number 4

Injected Water	Tube #	W_i (cc)	V_{oil} Produced		W_i (PV)	RF (%)
			Per tube	Cumulative		
	0	0	0	0	0	0.00
SW	1.1	1.42	0.9	0.9	0.2	21.43
	1.2	0.67	0.3	1.2	0.3	28.57
	1.3	0.83	0.3	1.5	0.4	35.71
	1.4	0.83	0.1	1.6	0.5	38.10
	1.5	0.83	0	1.6	0.7	38.10
	1.6	0.83	0	1.6	0.8	38.10
	1.7	0.83	0	1.6	0.9	38.10
	1.8	51	0.5	2.1	8.4	50.00
	1.9	100	0.35	2.45	23.0	58.33
	1.10	100	0	2.45	37.6	58.33
SW x2SO4	2.1	15	0	2.45	39.7	58.33
	2.20	26	0.1	2.55	43.5	60.71
	2.3	50	0	2.55	50.8	60.71
SW x6SO4	3.1	15	0.01	2.56	53.0	60.95
	3.2	50	0.05	2.61	60.3	62.14
	3.3	50	0	2.61	67.6	62.14

Figure 3.21 shows the oil recovery factor for the three different injected brines versus the pore volume injected.
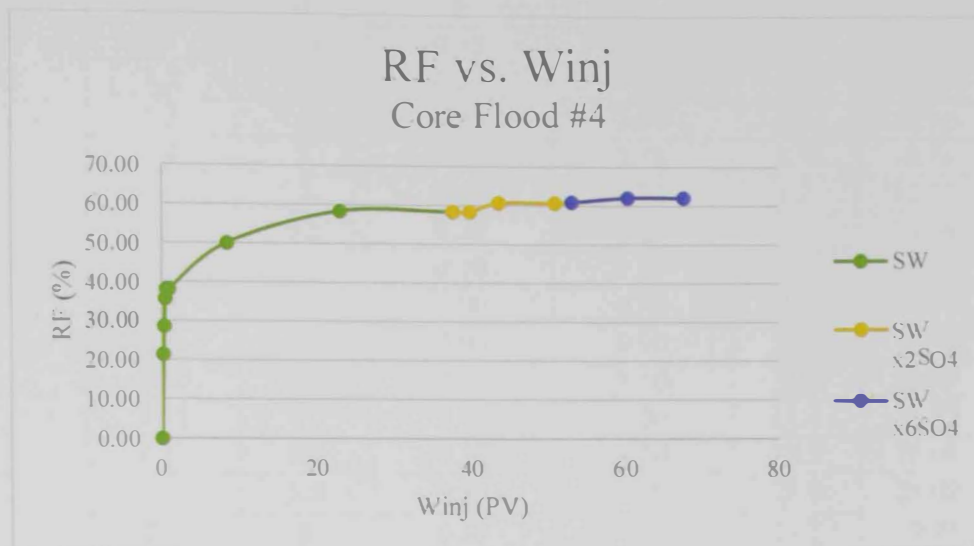
Figure 3.21: Recovery factor versus pore volume injected for LSWF number 4

The obtained values of effective permeability and effluent properties were similar to what was measured during for the first LSWF experiment.

3.5.5 LSWF Number 5 (Brine Category 5)

No incremental oil recovery was obtained by spiking the sulfate content of seawater or its dilutions. Thus, the fifth experiment was designed exclusively to investigate the effect of seawater dilution. In this experiment, core sample number 13 was flooded sequentially with seawater, 10 and 50 times dilutions. The results of these LSWF experiments are listed in table 3.13.

Table 3.13: Core flooding results for LSWF number 5

| Injected Water | Tube # | W_i (cc) | V_{oil} Produced | | W_i (PV) | RF (%) |
			Per tube	Cumulative		
SW	0	0	0	0	0	0
	1.1	1.3	0.35	0.35	0.2	6.36
	1.2	1.8	0.25	0.60	0.4	10.91
	1.3	1.95	0.00	0.60	0.6	10.91
	1.4	2	0.10	0.70	0.9	12.73
	1.5	2	0.00	0.70	1.2	12.73
	1.6	5.5	0.20	0.90	1.9	16.36
	1.7	5	0.00	0.90	2.5	16.36
	1.8	5.5	0.00	0.90	3.2	16.36
	1.9	12	0.00	0.90	4.7	16.36
	1.10	25	0.20	1.10	7.9	20.00
	1.11	51	0.10	1.20	14.4	21.82
	1.12	101	0.10	1.30	27.3	**23.64**
SW/10	2.1	5.5	0.30	1.60	28.0	29.09
	2.2	6	0.10	1.70	28.7	30.91
	2.3	9.5	0.50	2.20	29.9	40.00
	2.4	50	0.10	2.30	36.3	41.82
	2.5	50	0.00	2.30	42.7	**41.82**
SW/50	3.1	5.5	0.00	2.30	43.4	41.82
	3.2	14	0.00	2.30	45.2	41.82
	3.3	52	0.00	2.30	51.8	**41.82**

The results indicated that a significant increase (almost double) in oil recovery could be obtained when 10-times-diluted seawater was injected, as illustrated in figure 3.22.
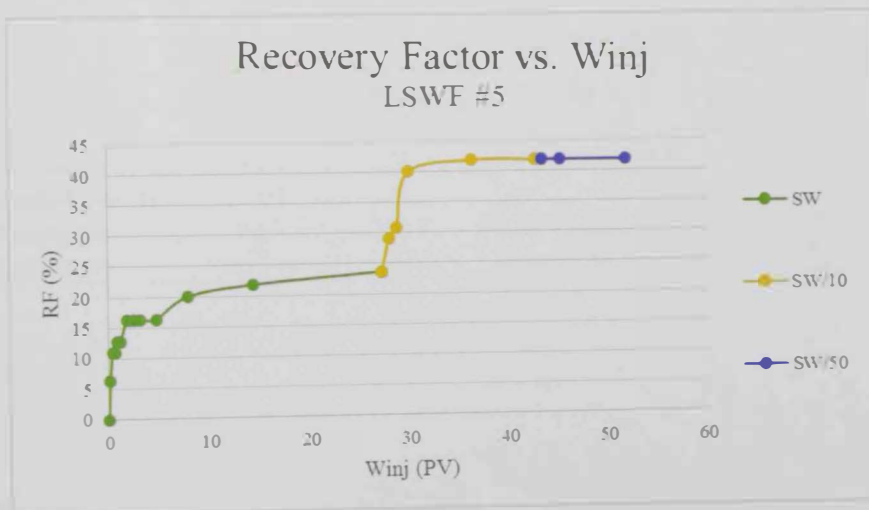
Figure 3.22: Recovery factor versus pore volume injected for LSWF number 5

Flooding the core sample with more diluted brines was also accompanied by a significant reduction in endpoint effective permeability to water. Figure 3.23 shows the values end point effective permeability for each injected brine.

Figure 3.23: End-point effective permeability for LSWF #5

This could best explain the dissolution phenomenon when it is put together with effluent properties before and after the experiment as listed in table 3.14.

Table 3.14: Effluent properties for LSWF number 5

Parameter	Unit	SW		SW/10		SW/50	
		Before	After	Before	After	Before	After
pH	log(mol/L)	7.32	7.08	7.25	7.35	6.70	7.22
Turbidity	NTU	0	7	0	54	0	28
Suspended Solids	mg/L	0	11	0	64	0	25
Hardness	mg/L	2851	3007	275	1022	60	986
Resistivity	mΩ-m	77	75	622	391	2755	1755

Similar to previous flooding experiments, no specific trend could be found between the pH and the crude oil recovery. Figure 3.24 shows the pH value of the injected brines before and after the experiment.
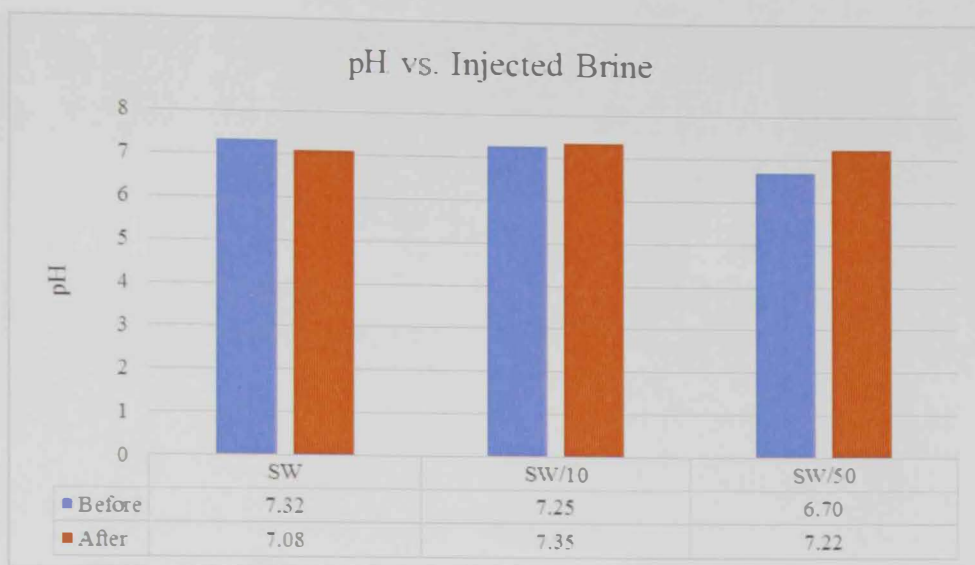
Figure 3.24: pH value of effluents for LSWF number 5

The dissolution phenomenon can be perfectly justified using the values of the brine turbidity and the amount of total suspended solids before (totally transparent with no suspended solids) and after, as presented in figure 3.25.
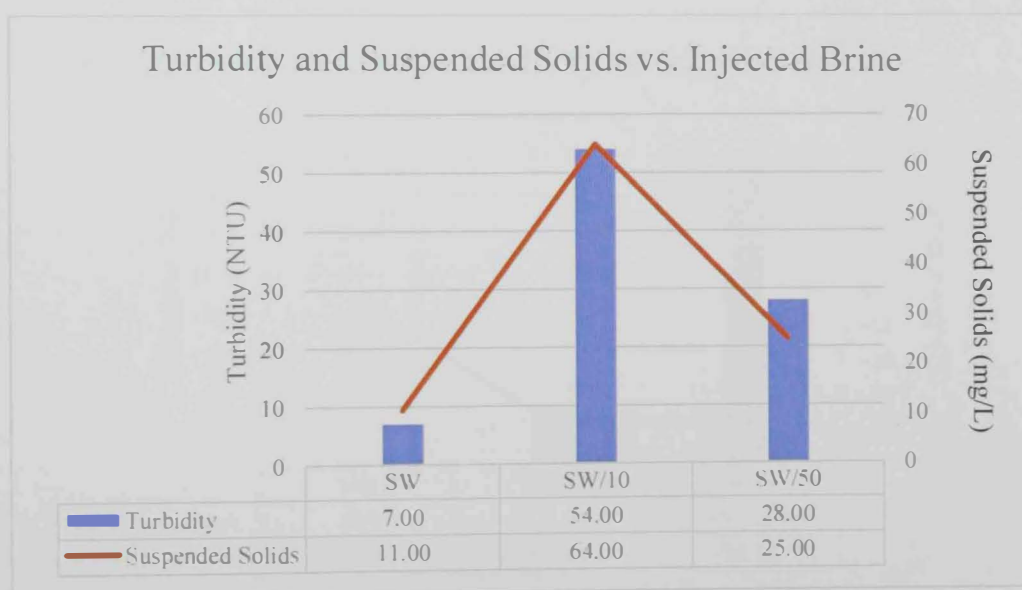
Figure 3.25: Turbidity and Total Suspended Solids for LSWF number 5

The above results indicate that the water turbidity and total suspended solids increased significantly for the 10-times-diluted seawater sample: the injected brine that could result in maximum oil recovery. This is best observed in figure 3.26.

Figure 3.26: Turbidity of the injected brines before and after LSWF #5

The dissolution hypothesis was also verified using both values of brine resistivity and water hardness as presented in figure 3.27.
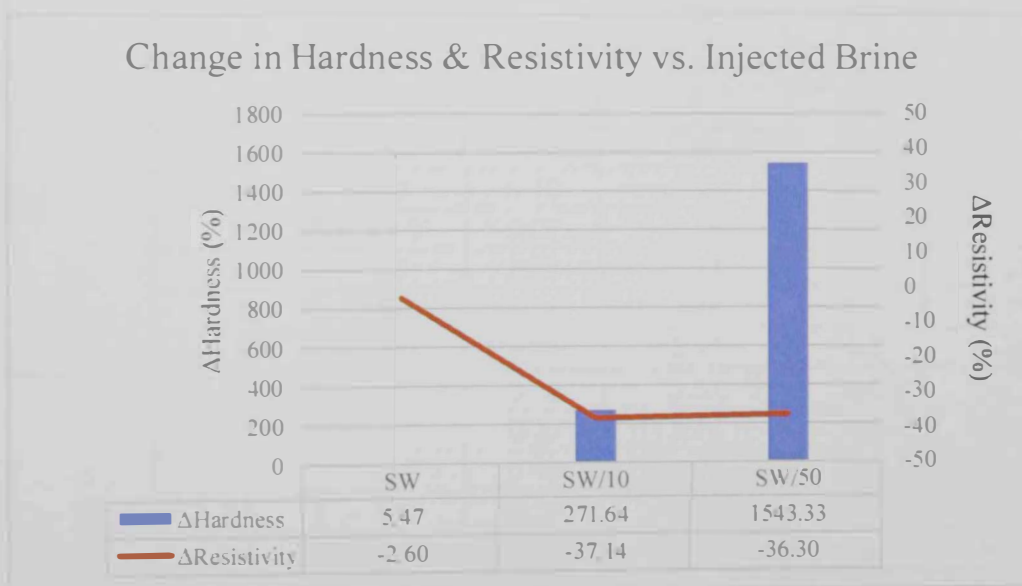
Figure 3.27: Change in Water Hardness and Resistivity for LSWF number 5

The results indicate that injecting diluted seawater into the formation have resulted in an increase of calcium concentration and salinity of the water.

3.5.6 LSWF Number 6 (IW Followed by SW/1)

Based on the results of low salinity water flooding experiments 1 to 5, it is concluded that the highest recovery factor can be obtained when 10 times diluted seawater (with no spike in sulfate concentration) is injected into the core plug. The last LSWF experiment was designed to assess the potential of the selected smart brine in increasing the oil recovery in a rock that has been already flooded with injection water (IW). The sixth flooding experiment was conducted on core number 9. The results of this LSWF experiment are listed in table 3.15.

Table 3.15: Core flooding results for LSWF number 6

Injected Water	Tube #	W_i (cc)	V_{oil} Produced		W_i (PV)	RF (%)
			Per tube	Cumulative		
	0	0	0	0	0	0
	1.1	2.2	0.47	0.47	0.3	10.22
	1.2	1.22	0.55	1.02	0.5	22.17
	1.3	1.25	0.23	1.25	0.6	27.07
	1.4	1.2	0.38	1.62	0.8	35.22
	1.5	1.1	0.10	1.72	0.9	37.39
IW	1.6	2	0.15	1.87	1.2	40.65
	1.7	5.5	0.25	2.12	1.9	46.09
	1.8	5	0.10	2.22	2.6	48.26
	1.9	14	0.10	2.32	4.4	50.43
	1.10	13.5	0.03	2.35	6.2	50.98
	1.11	25	0.03	2.37	9.5	51.52
	1.12	50	0.08	2.45	16.1	53.15
	1.13	100	0.03	2.47	29.2	**53.70**
	2.1	2	0.10	2.57	29.5	55.87
	2.2	5.5	0.20	2.77	30.2	60.22
SW/10	2.3	13.5	0.30	3.07	32.0	66.74
	2.4	26	0.10	3.17	35.4	68.91
	2.5	50	0.05	3.22	42.0	70.00
	2.6	100	0.00	3.22	55.2	**70.00**

Results indicate that injecting 10 times diluted seawater could increase the recovery factor by more than 15%. This can be best visualized in figure 3.28.
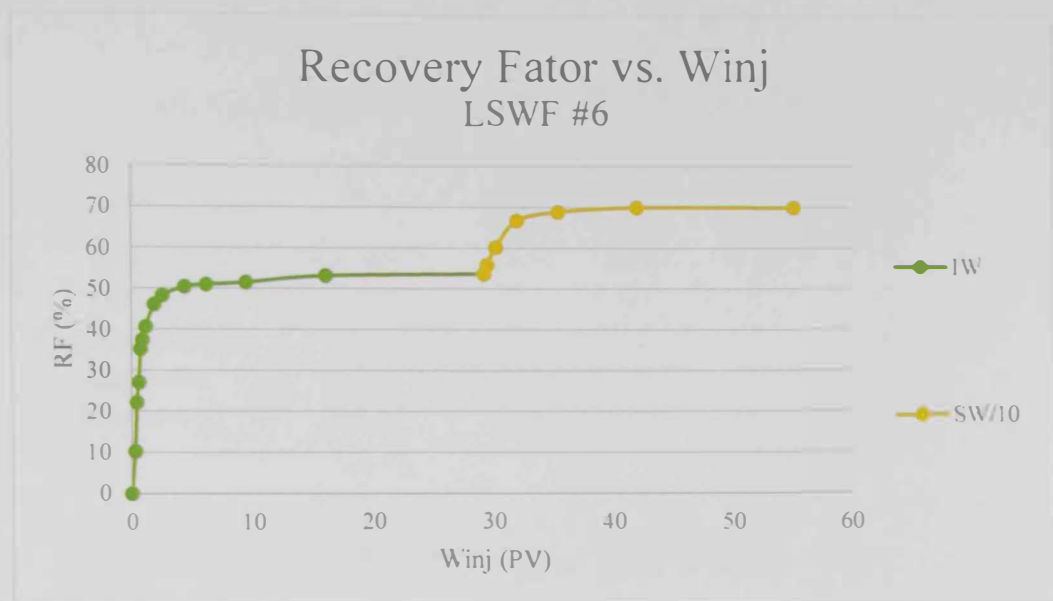
Figure 3.28: Recovery factor versus pore volume injected for LSWF number 6

Figure 3.29 shows the values of end point effective permeability for the injected brines.
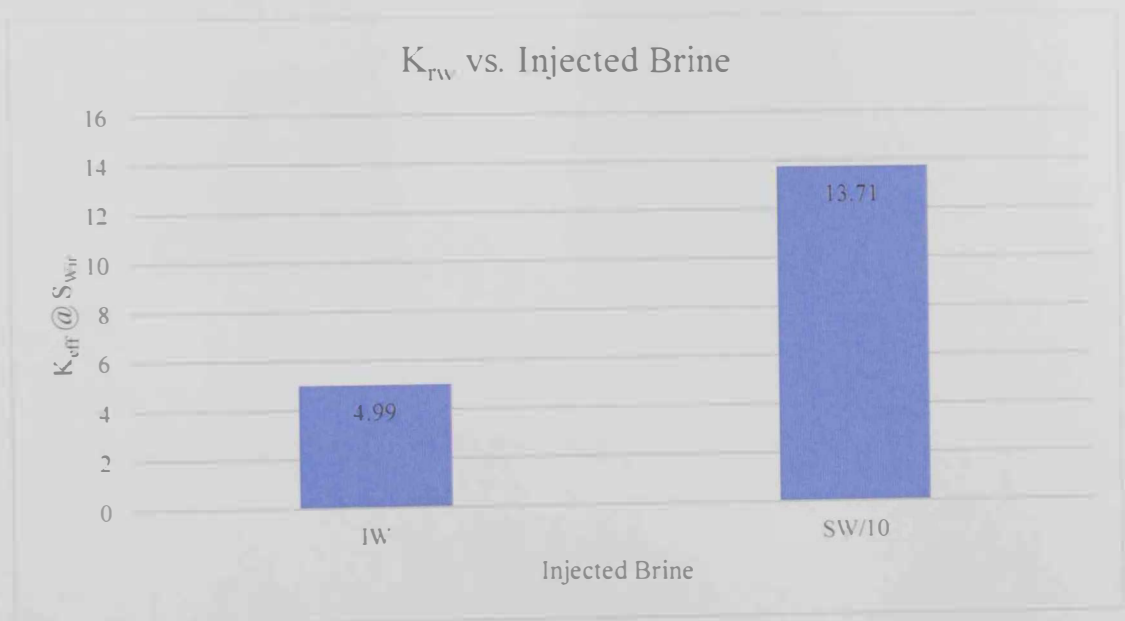
Figure 3.29: End-point effective permeability for LSWF #6

The results of end-point effective permeability along with the measured properties of effluents (presented in table 3.16) can be used to justify the dissolution mechanism behind the incremental oil recovery.

Table 3.16: Effluent properties for LSWF number 6

Parameter	Unit	IW		SW/10	
		Before	After	Before	After
pH	log(mol/L)	6.60	6.45	6.25	7.61
Turbidity	NTU	6	11	0	55
Suspended Solids	mg/L	0	15	0	68
Hardness	mg/L	24220	23657	275	1058
Resistivity	mΩ-m	35	36	622	318

Similarly, no relation between the brine acidity and incremental oil recovery was observed as presented in figure 3.30.

	IW	SW/10
Before	6.60	6.25
After	6.45	7.61
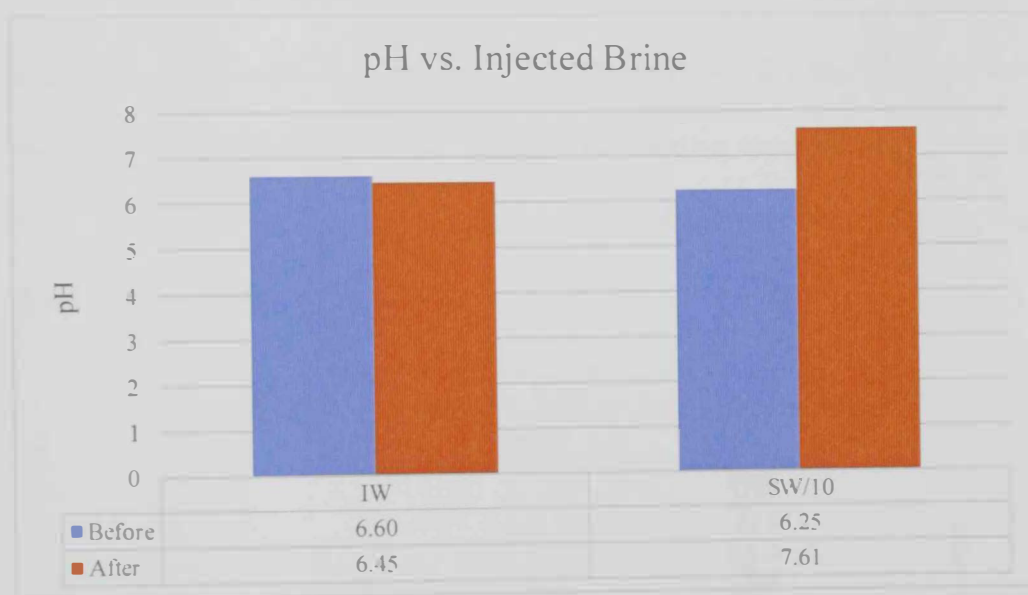
Figure 3.30: pH value of effluents for LSWF number 5

The significant increase in turbidity and the amount of total suspended solids in the 10-times-diluted seawater justified the rock dissolution occurrence. Figure 3.31 show the results of turbidity and total suspended solids in the injected brines.
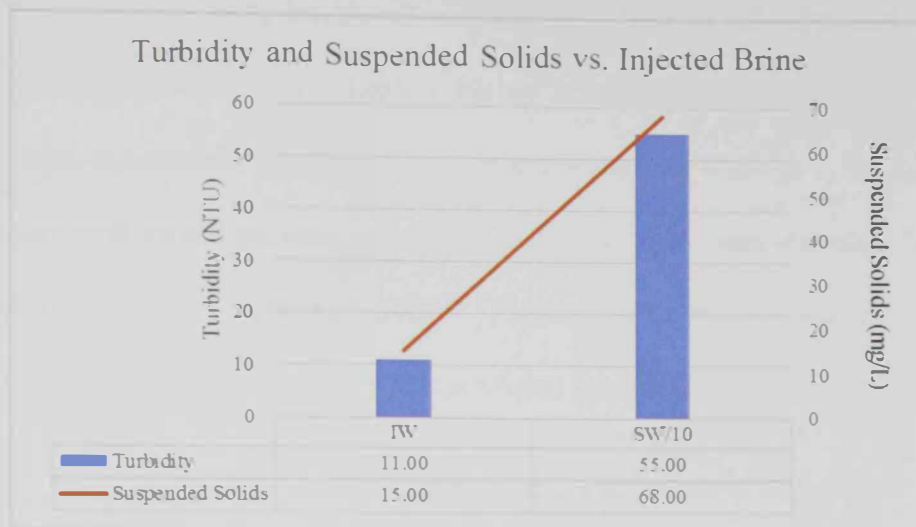
Figure 3.31: Turbidity and Total Suspended Solids for LSWF number 3

The same conclusion was obtained when the values of water hardness and brine resistivity were compared, before and after the flooding experiment as shown in figure 3.32. The salinity and calcium concentration significantly increased during the SW/10 flooding experiment.
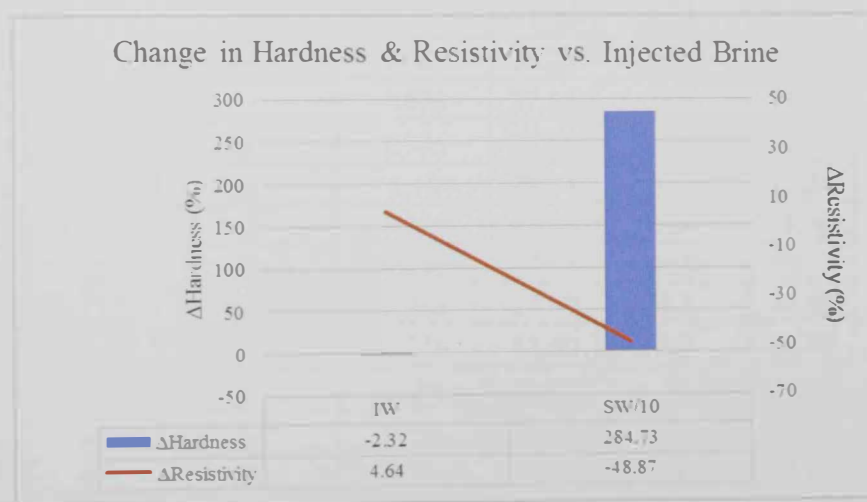
Figure 3.32: Change in Water Hardness and Resistivity for LSWF number 3

3.6 Spontaneous Imbibition Studies

The low acid number (AN) value of the oil and the insignificant effect of sulfate spiking on oil recovery induced us toward conducting the spontaneous imbibition/drainage experiments to evaluate the effect of dilution exclusively. As spontaneous experiments are usually highly affected by rock heterogeneity, three imbibition experiments were conducted on cores samples number 5, 16 and 24 in the same temperature and pressure conditions. All three cores were sequentially placed in injection water (IW), SW and SW/10. The results of the spontaneous imbibition experiments for all three core samples are listed in table 3.17.

Table 3.17: Results of spontaneous imbibition experiments

| Day	Brine	Comulative Day	Core #5		Core #16		Core #24	
			Volume	RF	Volume	RF	Volume	RF
0		0	0	0.00	0	0.00	0	0.00
1		1	0.2	5.13	0.075	2.14	0.05	1.25
2		2	0.4	10.26	0.15	4.29	0.1	2.50
3	IW	3	0.5	12.82	0.2	5.71	0.15	3.75
5		5	0.6	15.38	0.3	8.57	0.2	5.00
8		8	0.7	17.95	0.3	8.57	0.2	5.00
10		10	0.7	17.95	0.3	8.57	0.2	5.00
1		11	0.85	21.79	0.375	10.71	0.275	6.88
3		13	0.95	24.36	0.45	12.86	0.325	8.13
5	SW	15	1.025	26.28	0.475	13.57	0.35	8.75
8		18	1.075	27.56	0.5	14.29	0.375	9.38
10		20	1.075	27.56	0.5	14.29	0.375	9.38
1		21	1.16	29.74	0.59	16.86	0.445	11.13
3		23	1.225	31.41	0.66	18.86	0.475	11.88
5	SW/10	25	1.255	32.18	0.68	19.43	0.515	12.88
8		28	1.275	32.69	0.7	20.00	0.525	13.13
10		30	1.275	32.69	0.7	20.00	0.525	13.13
1		31	1.29	33.08	0.715	20.43	0.54	13.50
3		33	1.31	33.59	0.735	21.00	0.56	14.00
5	SW/50	35	1.32	33.85	0.745	21.29	0.57	14.25
8		38	1.325	33.97	0.75	21.43	0.575	14.38
10		40	1.325	33.97	0.75	21.43	0.575	14.38

Figure 3.33 provides a graphical representation of spontaneous imbibition studies.

Recovery Factor vs. Time
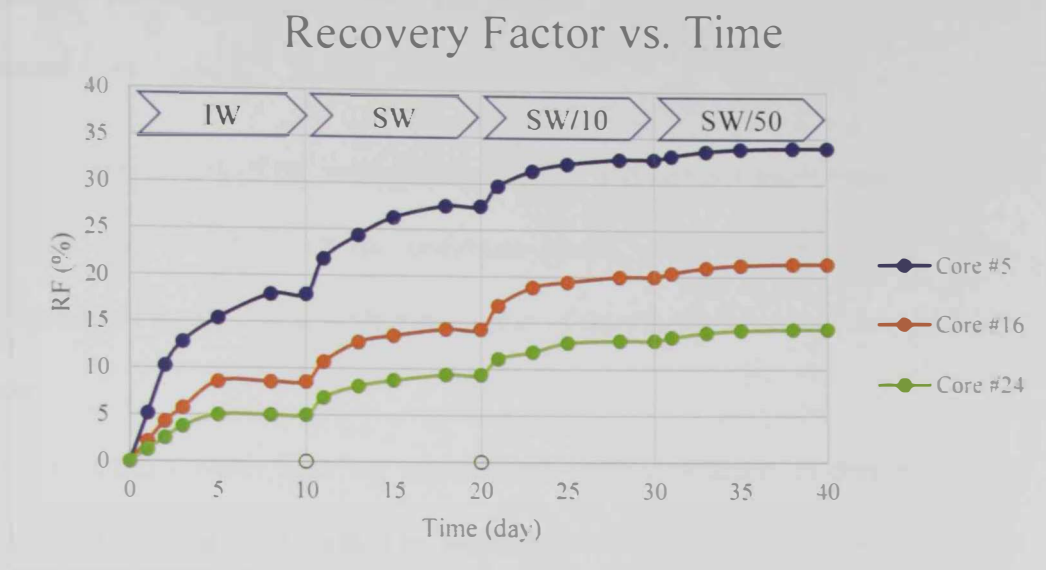
Figure 3.33: RF as a function of time for various spontaneous imbibition experiments

The results spontaneous imbibition experiments indicate that the dilution of the injected brine can alter the wettability toward a more oil-wetting state and positively effect on the oil recovery. It was observed that the ten-times-diluted seawater can increase the oil recovery by 7 to 15%. Moreover, excessive dilutions of the seawater showed no significant effect wettability alteration.

Chapter 4: Conclusion and Recommendation

4.1 Conclusion

Based on the results of the experimental work conducted, the following conclusions were made:

1. Based on the results of the static studies of IFT and contact angle measurements, seawater was found to be the optimum smart water. Increasing the sulfate concentration resulted in a further reduction of interfacial tension between oil and water.

2. The low salinity water flooding experiments were conducted on core plugs that were in intermediate-wet state. The wettability of the cores was explained by the low acid number of the oil (0.07 mg KOH/g of oil) and the results of oil flooding experiments after 40 days of aging at 80 °C.

3. Spiking the sulfate content of seawater showed no effect on wettability alteration. This was justified by the first four sequential LSWF experiments conducted at reservoir temperature (255 °F) conditions.

4. Low salinity water flooding showed a positive potential in increasing the oil recovery for Asab oil field. This conclusion is based on the results of the fifth LSWF experiment. The incremental recovery obtained by injecting low salinity brine was significant as it could approximately double the volume of oil produced.

5. Thin section examination studies showed that the rock samples are composed of nonskeletal alochem grains that are cemented together with sparry calcite.

6. The mechanism behind low salinity water flooding was found to be rock dissolution. The dissolved minerals seem to be the calcite cement in the rock structure.

7. Absolute permeability of the core samples that were flooded by low salinity water flooding (50-60 pore volumes injected) was increase by a factor of 8 to 10. Rock dissolution was suggested to be the reason behind this observation.

8. The 10 times diluted seawater (6250 ppm) was shown to have the optimum salinity and could result in 15% extra oil recovery when it was injected in the tertiary recovery stage.

9. Farther dilutions was found to be unnecessary as they could not result in any incremental oil recovery.

10. No correlation between the acidity of brine and oil recovery could be concluded.

11. The results of spontaneous imbibition experiments indicated that dilution can alter the wettability of the rock toward a more oil-wetting state. Oil recovery was increased by 6 to 15% for various core plugs when the ten-times-diluted seawater was used. It was also observed that the fifty-times-diluted seawater did not result in any significant improvement in the oil recovery.

4.2 Recommendation

1. Further experiments should be conducted to study the effect of sulfate concentration on core plugs that are saturated with oil that have high acid numbers.

2. To study the dissolution process, it is recommended to monitor the pressure drop across the core continuously and measure the ionic composition and TSS of the effluents at different pore volumes injected.

References

Al-adasani, A., Bai, B., & Wu, Y.-S. (2012). Investigating Low Salinity Waterflooding Recovery Mechanisms in Carbonate Reservoirs. Society of Petroleum Engineers. https://doi.org/10.2118/155560-MS

Al Harrasi, A., Al-maamari, R. S., & Masalmeh, S. K. (2012). Laboratory Investigation of Low Salinity Waterflooding for Carbonate Reservoirs. Society of Petroleum Engineers. https://doi.org/10.2118/161468-MS

Al-Attar, H. H., Mahmoud, M. Y., Zekri, A. Y., Almehaideb, R., & Ghannam, M. (2013). Low-salinity flooding in a selected carbonate reservoir: experimental approach. *Journal of Petroleum Exploration and Production Technology, 3*(2), 139–149. https://doi.org/10.1007/s13202-013-0052-3

Alotaibi, M. B., Azmy, R., & Nasr-El-Din, H. A. (2010). Wettability Challenges in Carbonate Reservoirs. Presented at the SPE Improved Oil Recovery Symposium, Society of Petroleum Engineers. https://doi.org/10.2118/129972-MS

Arps, J. J. (1967). Statistical Analysis of Crude Oil Recovery and Recovery Efficiency. *American Petroleum Institute., Bulletin D14.*

Austad, T., Shariatpanahi, S. F., Strand, S., Black, C. J. J., & Webb, K. J. (2012). Conditions for a Low-Salinity Enhanced Oil Recovery (EOR) Effect in Carbonate Oil Reservoirs. *Energy & Fuels, 26*(1), 569–575. https://doi.org/10.1021/ef201435g

Bagci, S., Kok, M. V., & Turksoy, U. (2001). Effect Of Brine Composition On Oil Recovery By Waterflooding. *Petroleum Science and Technology, 19*(3–4), 359–372. https://doi.org/10.1081/LFT-100000769

Boneau, D. F., & Clampitt, R. L. (1977). A Surfactant System for the Oil-Wet Sandstone Of the North Burbank Unit. *Journal of Petroleum Technology, 29*(5), 501–506. https://doi.org/10.2118/5820-PA

Dake, L. P. (2001). *The practice of reservoir engineering* (Rev. ed). Amsterdam ; New York: Elsevier.

Fundamentals of Wettability (Oilfield Review) | Schlumberger. (n.d.). Retrieved August 31, 2016, from http://www.slb.com/resources/publications/industry_articles/oilfield_review/2007/or2007sum04_wettability.aspx

Green, D. W., & Willhite, G. P. (1998). *Enhanced oil recovery.* Richardson, TX: Henry L. Doherty Memorial Fund of AIME, Society of Petroleum Engineers.

Greg Adams, Faouzi Aloulou, Lori Aniti, Erin Boedecker, William Brown, Nicholas Chase, Michael Cole, Troy Cook, David Daniels, Mindi Farber-DeAnda, Craig Federhen, Michael Ford, Adrian, Geagla, Patricia Hutchins, Scott Jell, Slade Johnson, Jeff Jones, Ari Kahan, Diane Kearney, Augustine Kwon, Danielle Lowenthal-Savy, David Manowitz, Nilay Manzagol, John Maples, Cara Marcy, Laura Martin, Fred Mayes, Michael L. Mellish, Michael Morris, Brian, T. Murphy, Chris Namovicz, Kelly Perl, Chetha Phang, John Powell, Anthony Radich, Elizabeth Sendich, Charles L. Smith, Kay Smith, & John Staub, and Peggy Wells. (2016). *International Energy Outlook 2016* (No. IEO2016).

Gupta, R., Smith, G. G., Hu, L., Willingham, T., Lo Cascio, M., Shyeh, J. J., & Harris, C. R. (2011). Enhanced Waterflood for Carbonate Reservoirs - Impact of Injection Water Composition. Society of Petroleum Engineers. https://doi.org/10.2118/142668-MS

Hognesen, E. J., Strand, S., & Austad, T. (2005). Waterflooding of preferential oil-wet carbonates: Oil recovery related to reservoir temperature and brine composition. Society of Petroleum Engineers. https://doi.org/10.2118/94166-MS

Jassim Abubacker Ponnambathayil. (2016). *Contact Angle And Ift Measurements Of Smart Water At Elevated Temperatures And Pressures For Evaluating Wettability In A Selected Carbonate Reservoir In The Uae*. UAE University, Al Ain, Abu Dhabi.

Lager, A., Webb, K. J., Collins, I. R., & Richmond, D. M. (2008). LoSal Enhanced Oil Recovery: Evidence of Enhanced Oil Recovery at the Reservoir Scale. Society of Petroleum Engineers. https://doi.org/10.2118/113976-MS

Moeini, F., Hemmati-Sarapardeh, A., Ghazanfari, M.-H., Masihi, M., & Ayatollahi, S. (2014). Toward mechanistic understanding of heavy crude oil/brine interfacial tension: The roles of salinity, temperature and pressure. *Fluid Phase Equilibria, 375*, 191–200. https://doi.org/10.1016/j.fluid.2014.04.017

RezaeiDoust, A., Puntervold, T., Strand, S., & Austad, T. (2009). Smart Water as Wettability Modifier in Carbonate and Sandstone: A Discussion of Similarities/Differences in the Chemical Mechanisms. *Energy & Fuels, 23*(9), 4479–4485. https://doi.org/10.1021/ef900185q

Robertson, E. P. (2007). Low-Salinity Waterflooding to Improve Oil Recovery-Historical Field Evidence. Society of Petroleum Engineers. https://doi.org/10.2118/109965-MS

Romanuka, J., Hofman, J., Ligthelm, D. J., Suijkerbuijk, B., Marcelis, F., Oedai, S., … Austad, T. (2012). Low Salinity EOR in Carbonates. Society of Petroleum Engineers. https://doi.org/10.2118/153869-MS

Schlumberger. (2007). *Schlumberger Market Reveiw 2007*.

Sheng, J. J. (2014). Critical review of low-salinity waterflooding. *Journal of Petroleum Science and Engineering*, *120*, 216–224. https://doi.org/10.1016/j.petrol.2014.05.026

Strand, S., Høgnesen, E. J., & Austad, T. (2006). Wettability alteration of carbonates— Effects of potential determining ions (Ca2+ and SO42−) and temperature. *Colloids and Surfaces A: Physicochemical and Engineering Aspects*, *275*(1– 3), 1–10. https://doi.org/10.1016/j.colsurfa.2005.10.061

The South East. (n.d.). Retrieved August 29, 2016, from http://adcoae1:1003/en/Operations/AsabSahilShahFields/Pages/Overview.asp x

Tiab, D., & Donaldson, E. C. (2016). *Petrophysics: theory and practice of measuring reservoir rock and fluid transport properties* (4. ed). Amsterdam: Elsevier/GPP Gulf Professional Publ.

Tzimas, E., Georgakaki, A., Garcia-Cortes, C., & Institute for Energy (European Commission). (2005). *Enhanced oil recovery using carbon dioxide in the European energy system*. Luxembourg: Publications Office. Retrieved from http://bookshop.europa.eu/uri?target=EUB:NOTICE:LDNA21895:EN:HTM L

Webb, K. J., Black, C. J. J., & Tjetland, G. (2005). A Laboratory Study Investigating Methods for Improving Oil Recovery in Carbonates. International Petroleum Technology Conference. https://doi.org/10.2523/IPTC-10506-MS

Yildiz, H. O., & Morrow, N. R. (1996). Effect of brine composition on recovery of Moutray crude oil by waterflooding. *Journal of Petroleum Science and Engineering*, *14*(3–4), 159–168. https://doi.org/10.1016/0920-4105(95)00041-0

Yousef, A. A., Al-Saleh, S., Al-Kaabi, A. U., & Al-Jawfi, M. S. (2010). Laboratory Investigation of Novel Oil Recovery Method for Carbonate Reservoirs. Society of Petroleum Engineers. https://doi.org/10.2118/137634-MS

Zekri, A. Y., Nasr, M. S., & Al-Arabai, Z. I. (2011). Effect of LoSal on Wettability and Oil Recovery of Carbonate and Sandstone Formation. International Petroleum Technology Conference. https://doi.org/10.2523/IPTC-14131-MS

Zhang, P., & Austad, T. (2005). The Relative Effects of Acid Number and Temperature on Chalk Wettability. Society of Petroleum Engineers. https://doi.org/10.2118/92999-MS

Zhang, P., & Austad, T. (2005). Waterflooding in chalk: Relationship between oil recovery, new wettability index, brine composition and cationic wettability modifier. Society of Petroleum Engineers. https://doi.org/10.2118/94209-MS

Zhang, Y., & Morrow, N. R. (2006). Comparison of Secondary and Tertiary Recovery With Change in Injection Brine Composition for Crude-Oil/Sandstone Combinations. Society of Petroleum Engineers. https://doi.org/10.2118/99757-MS

Appendix A: Brine Calculations

The ionic composition of all SW, FW and IW were measured and reported by ADNOC using ICP (anaions) and Ion chromatography (for cataions). Ionic balance calculations were then attempted to balance the brine compositions prior to brine preparations. The balancing was done using addition or subtraction of either Sodium or Chlorine ions, as they have proven to be non-determining ions in wettability alteration (Alotaibi et al., 2010). The calculations were done using regression analysis to achieve the "perfect" ionic balance value of 1.0. Table A.1 shows the example calculation for seawater:

Table A.1: Example ionic balance calculation for seawater

CATIONS ANALYSED (mg/L)		ANIONS ANALYSED (mg/L)		CATIONS ANALYSED (meq/L)		ANIONS ANALYSED (meq/L)	
Na+	19,054.00	Cl -	35,835.77	Na+	0.8288	Cl -	1.0108
Ca++	690.00	SO4 -	3,944.00	Ca++	0.0344	SO4 -	0.0411
Mg++	2,132.00	HCO3 -	123.00	Mg++	0.1754	HCO3 -	0.0020
K+	672.00	CO3 -		K+	0.0172	CO3 -	
Ba++		OH3-		Ba++		OH3-	
Fe++		I-		Fe++		I-	
Sr++	0.00	NO3-	0.00	Sr++		NO3-	0.0020
Li+		Br-	0.00	Li+		Br-	
				Sum	1.06	Sum	1.06
				Ratio of Cations to Anions =>			1

The amount of salts required to prepare the water with the specific ionic compositions was then calculated using an excel spreadsheet previously developed by Core Laboratories International. Table A.2 shows an example of these calculations for seawater. The most right hand column of the tables represents the order of salts added (starting with divalent less electronegative ions and ending with NaCl).

Table A.2: Example calculations of the salts needed to prepare seawater synthetically

Well:	SB-0567
Field:	Asab
Formation:	
Location:	UAE
Wt. of 10.078cc Brine:	10.47891
Concentration (ppm):	60,061
Specific Gravity (gm/cc):	1.0398

| CHEMICALS	1 LITRE mg	1 LITRE gm	2 LITRE gm	Sequence
NaHCO3 (Anhy)	169.35	0.17	0.34	5
Na2CO3 (Anhy)	0.00	0.00	0.00	
Na2SO4 (Anhy)	5831.99	5.83	11.66	3
NaCl	43520.06	43.52	87.04	6
CaCl2 (Anhydrous)	1910.68	1.91	3.82	
CaCl2 2 H2O	2530.99	2.53	5.06	2
MgCl2.6H2O	17833.33	17.83	35.67	1
KCl	1281.30	1.28	2.56	4
SrCl2.6H2O	0.00	0.00	0.00	
LiCl	0.00	0.00	0.00	
BaCl2.2H2O	0.00	0.00	0.00	
CaCl2 6 H2O	3771.54	3.77	7.54	

Appendix B: Brine Preparation

The following procedure has been used for preparation of brine:

1. Prepare a volumetric flask washed with Deionized water, with the required volume 1, 2 or 5 liters.

2. Fill half of the volumetric flask (approximately) with deionized water.

3. Carefully place a magnetic stirrer in the flask and place the flask on the stirring pad and switch it on.

4. Use a funnel to add the required amount of salts following the orders on the excel spreadsheet.

5. Fill the volumetric flask to the required volume of 1, 2 or 5 liters (taking the volume of the stirrer into account).

6. Keep stirring until all the salts are dissolved.

7. Prepare a clean side-arm flask, a vacuum line, filtration funnel and 5 μm filter paper.

8. Gently place a magnetic stirrer in the side-arm flask.

9. Place the filter paper on the filtration funnel and gently pour the brine in the funnel as presented in figure B.1.a. Make sure that the sufficient vacuum pressure is applied through side-arm of the flask and the stirrer is on.

10. When brine is completely transferred, remove the funnel and place a rubber bung on top of the side-arm flask as presented in figure B.1.b. Turn both the vacuum and stirrer on for 2-3 minutes.

11. Quality check the prepared brine by measuring the resistivity of the brine and comparing it with the equivalent NaCl resistivity at room temperature(Tiab & Donaldson, 2016).
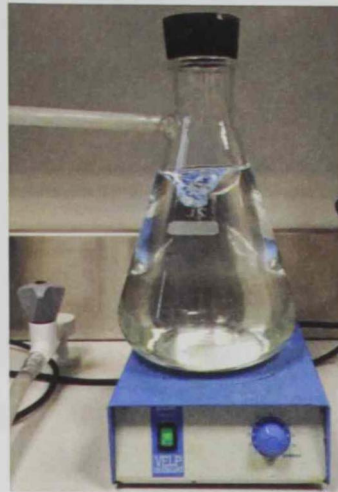
Figure B.1: a) Brine filtration. b) Brine degasification

12. Measure the density and viscosity of the prepared brine using a Pycnometer and Canon-Fenske respectively.

13. Pour the prepared brine in a sealed container and label it accordingly.

Appendix C: Dilution and Sulfate Spiking

Dilution

All the diluted waters were prepared using seawater as the base water of the dilution. The calculations were done using the dilution equation as follows:

$$C_1 V_1 = C_2 V_2$$

Where:

C_1 = concentration of the sea water (ppm)

V_1 = required volume of seawater (ml)

C_2 = required concentration of the new solution (ppm)

V_2 = required volume of the new water (ml)

Sulfate Spiking

The spiking was done by adding of sodium sulphate (Na_2SO_4) salt. Although the addition of sulfate in the form of sodium sulfate increases the amount of sodium in the solution, this increase was insignificant as sulfate has proven to be a non-determining ion in wettability alteration (Alotaibi et al., 2010). Molar masses of sodium and sulphate are 23 g/mol and 96 g/mol, respectively. This means that 1 mole of Na_2SO_4 weighs 142 g/mol. In other words, 0.479 grams of Sodium ion is added to the solution per gram of spiked sulfate. Two-time and six-time spikings were prepared based on the 885 mg/L of sulfate available in the formation water.

Two-times SO₄ Spiking: Having the seawater or any diluted brine twice-spiked means that the concentration of the sulfate was increased by 1,770 mg/L (the multiplier is 885mg/L of sulfate ion FW) of sulfate ion. In other word, the twice SO4 spiking was accomplished by addition of 2,618 mg/L of sodium sulfate to the solution.

Six-times SO₄ Spiking: Six-time sulfate spiking means that the concentration of sulfate in the brine is increased by 5,310 mg/L of sulfate ion. Six-time spiking was achieved by the addition of 7,854 grams of sodium sulfate into the original solution.

Appendix D: Core Preparation

Core Cleaning and Drying

A soxhlet extraction apparatus (shown in figure D.1) is used to extract the oil/brine from the core samples. In this method, toluene is gently boiled from a Pyrex flask; the vapor of toluene moves upward and condenses. The core plug is then submersed in the condensed toluene. When the level of the condensed fluid reaches the top of the siphon tune arrangement, the condensed toluene inside the soxhlet tube, are automatically emptied to the boiling flask (using siphon effect).
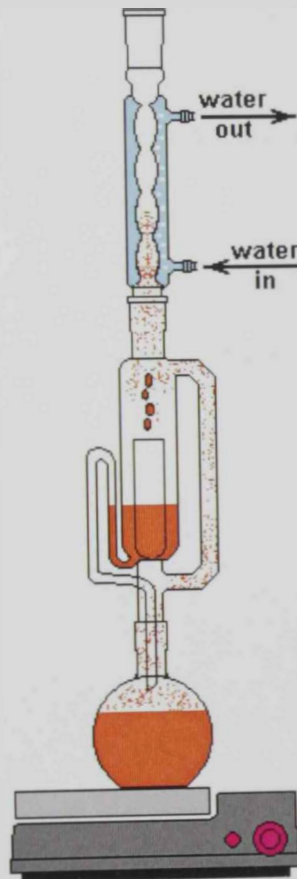

Figure D.1 Soxhlet apparatus used for extraction of the fluids

All core samples were kept in toluene (to extract the oil) and methanol (to extract the brine and salts). The cleaning is continued until not traces of oil can be observed under the UV light. The following procedure is used for core cleaning with soxhlet apparatus.

1. Core sample is placed in the soxhlet.

2. Soxhlet is then connected to the boiling flask.

3. The extracting fluid is poured into the soxhlet until the syphon level (this is repeated for at least 3 times/cycles).

4. Connect the soxhlet to the condenser and make sure the water is running through the condenser.

5. Place the set-up on the heating mantle and provide enough heat until a proper condensation rate is achieved.

6. Stop the soxhlet when the core is completely clean and no extra fluid can be extracted (usually after a duration of 7 to 10) days.

7. Place the cores in the oven at a temperature of 150 °C degrees (for sandstone cores. the temperature should be less than 100 °C) for 2 to 3 days.

Core Saturation

A method which is a combination of vacuum and pressure is used to saturate the core plugs with the formation brine. The apparatus in figure IV.2 is used in this stage of the experimental work.
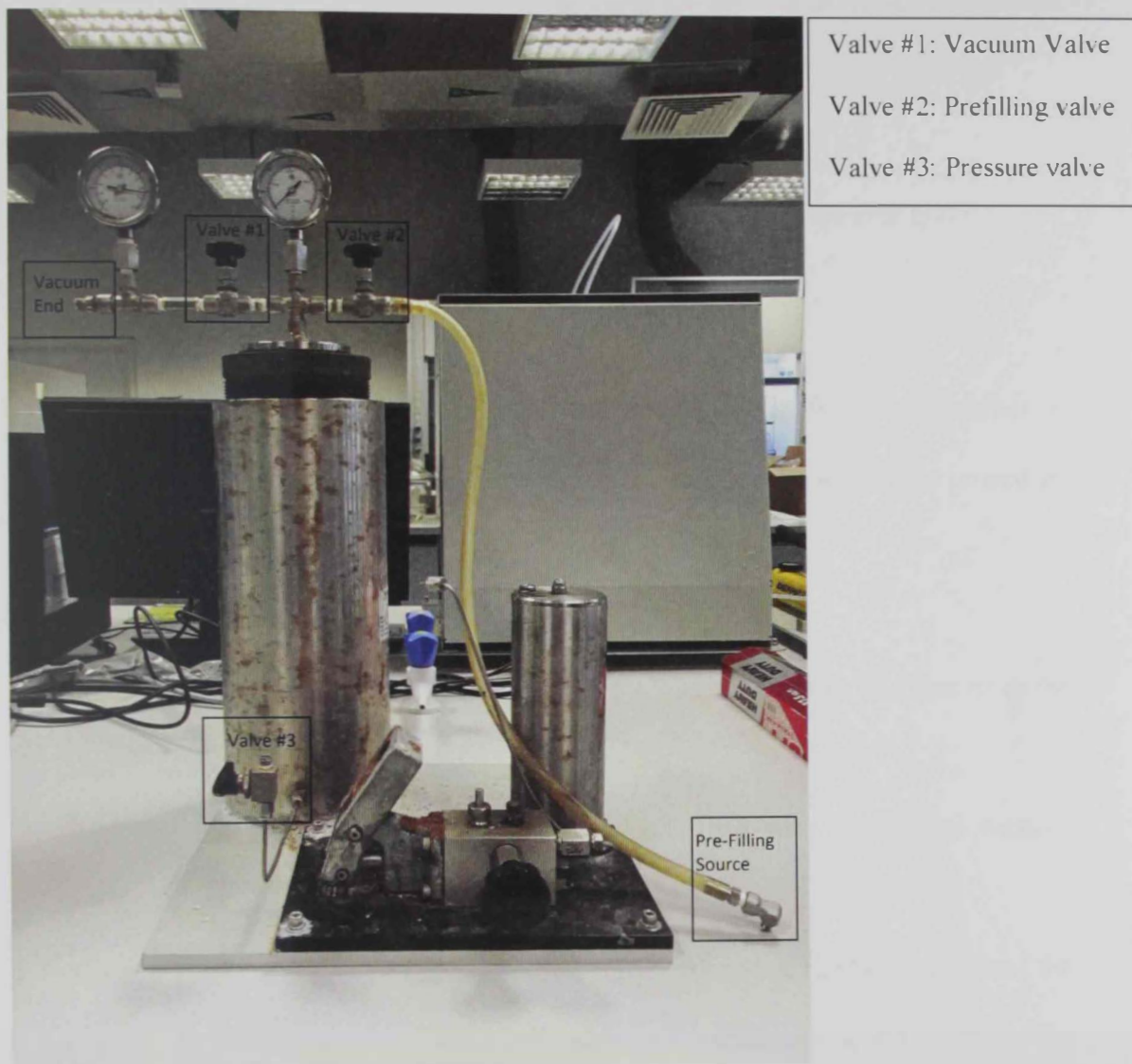

Figure D.2: Core saturation equipment

Vacuuming

In this stage of saturation experiment, vacuum pressure is used to empty the air from the pore space of the core plug.

1. In order to use less volume of formation water, fill half the saturation cylinder with core plugs that won't be used in the study.

2. Cover the cores with the formation brine completely.

3. Lay the cores that are to be saturated, on the cores that are used to fill the dead volume of the cylinder. Make sure that the cores are dry and completely out of the brine.

4. Put the lid of the chamber and close valve 2 and 3

5. Open the valve #1, connect it to the vacuum stream and let it run over night.

Pressurizing

After applying the vacuum pressure for an overnight, the chamber is completely filled and pressurized with formation brine. The following is the procedure used for pressurizing the core plugs with formation water.

1. Close the vacuum valve and pressure valve.

2. Put the prefilling source in the container filled with enough brine and then open the prefilling valve.

3. Wait for 20-30 minutes for the chamber to get filled with its original vacuum pressure.

Note: that this pressure of -1atm is only enough to saturate the larger pores of the core. In order to saturate the pores with very small radius, we need to increase the pressure of the chamber to approximately 3000 psi. Capillary pressure equation shows that in order to fill pores with small radiuses we need to impose high pressures:

$$P_c = \frac{2\sigma.\cos\theta}{r^2}$$

To pressurize the cell the injection pump shown in figure IV.3 was used:

Figure D.3: Injection pump

4. Close the "outlet" valve and open the "inlet" valve.

5. Press "RUN" to empty the storage chamber of the injection pump from distilled water.

6. Put the outlet or "refilling" line in our brine bottle (or container) and press "REFILL", until you see a message on the screen saying "FEFILLING COMPLETE".

   Note: In case of refilling in the middle of the process, make sure you FIRST close the outlet valve and then open the inlet valve. This is to prevent the back flushing of the water from the pressurized saturator to the refilling source.

7. Close the "inlet" valve and open the "outlet" Valve.

8. Connect the outlet of the injection pump to the pressure valve of the saturator (valve

#3)

9. Close all the valve of the saturator (valve 1 & 2) and open valve #3

10. Choose one of the "constant pressure" or "constant flowrate" methods and set your pressure or flow rate accordingly. Figure IV.4 shows the pump controller of the injection pump.

Figure D.4: Pump controller of the injection pump

11. Press run to fill and pressurize the saturator chamber to the required pressure of 3000 psig

    Note: Every once in a while, open the valve #2 of the saturator to bleed-of the air in the chamber. One RUN may not be enough, so it is usually required to refill the injection cylinder and run the injection again.

12. It is recommended to:

    Up to 2700 psig with 25 cc/min

    Up to 3000 psig with constant pressure

13. Once the pressure of 3000 psig is achieved, close the pressure valve of the saturator and let it stay under high pressure for a day.

14. Empty the cylinder of the injection pump and refill it with DI water.

Appendix E: Porosity and Permeability Measurement
Porosity and Permeability Measurements Using Nitrogen Gas

The Vinci PoroPerm Instrument (shown in figure V.1) is used to measure the density, porosity and permeability of the core sample using nitrogen gas.

Figure E.1: PoroPerm instrument used for porosity and permeability measurement

Porosity Measurement: The ideal gas law is used to calculate the pore volume and eventually, the grain density. A cell with a known volume is first filled with nitrogen gas and the pressure is recorded as P_{ref}. It is then connected to another cell containing the core plug, with an "unknown volume" (pore volume). The new pressure is measured as P_{exp} and is used to find the unknown volume (pore volume). The procedures to measure porosity is as follows:

1. Connect the plastic pressure input to the nitrogen gas cylinder.

2. Gently open the valve on the nitrogen cylinder until a pressure of approximately 150 psia is read on the gauge. Do not apply any confining pressure (confining pressure valve should be on Vent).

3. Click on "Update P_{atm}" to update and recalibrate the pressure sensors.

4. Place the core sample into the cell and fill the gap with the provided billets.

5. Select "GV+PV" and "No permeability measurement".

6. The only two valves used during Porosity measurements are Source valve and Matrix valve:

    a. Source valve should always be "ON"

    b. Matrix valve is opened/closed during the test

7. Keep the cell separated.

8. Input the following information into the software:

    a. Report name

    b. Operator name

    c. Sample name

    d. Weight (gram)

    e. Diameter (mm)

    f. Length (mm)

    g. Sample #

    h. Number of billets used

9. Press "START": Grain volume is calculated based on the dimensions.

10. Press "YES" (after checking the TO DO list): The first cell is filled with gas (pressure build up) and the cell pressure is then reported as "P_{ref}"

11. Turn the MATRIX CUP valve to "pressure" and press "OK".

12. Turn the MATRIX CUP valve to "Vent" and press "OK".

P_{exp} is then stabilized and recorded to calculate pore volume and grain density

Permeability measurements: The PoroPerm instrument can also be used to measure the permeability of a core sample using nitrogen gas. The software provided by Vinci Company has a built-in function to accounts for the slippage and Klinkenberg effects. and corrects the permeability values automatically. The procedure to measure permeability is as follows:

1   Connect the pressure input of the instrument to the gas cylinder and apply a confining pressure of 350-400 psia.

2   Select "No Volume Measurement" and "Kg Autoflow" on the screen.

3   The only valve used during permeability measurements is the "Confining Pressure" valve. The position of other valves should always be as:

   a.   Source valve should be "ON"

   b.   Matrix valve on "VENT"

   c.   Flow valve on "FPRWARD"

4   Click on "Update P_{atm}" to update and recalibrate the pressures sensors.

5   Input the followings into the software:

   a.   Report name

   b.   Operator name

   c.   Sample name

   d.   Diameter (mm)

   e.   Length (mm)

   f.   Sample #

6   Load the core plug in the cell and close it tightly.

7   Open the inlet and outlet valves.

8   Apply the confining pressure of 350-400 psi by turning the "CONFINING PRESSURE" valve to "PRESSURE".

9 Press "START", an excel spreadsheet will open and the dimensions and data will be recorded.

10 Press "YES" (after checking the TO DO list).The flow starts and it is scanned automatically each 15-30 seconds.

11 The software will report the calculated K value when it has stabilized.

Permeability Measurements Using Water Flooding

Core-holder and the core-flooding apparatus can be utilized to:

- Measure the absolute permeability by injecting brine in a core sample of fully saturated brine (S_w of 100%)

- Measure the recovery factor for various secondary/tertiary oil recovery techniques

- Construct the relative permeability curves

- Etc...

The flooding can be carried out using a conventional core holder, shown in figure E.2:

Figure E.2: Conventional core-holder

Permeability measurements: The procedure used for measurement of absolute permeability is as follows:

1. Gently place the core sample (at Sw of 100%) in the sleeve.

2. Place the flood head at one end and the end-stem at the other end of the core, as shown in figure E.3.
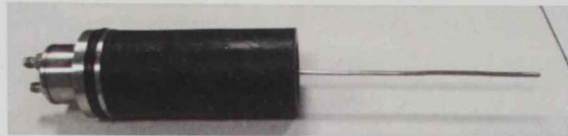

Figure E.3: A complete set-up of flood head, end-stem, core plug and sleeve

3. Lubricate the end-stem with some hydraulic oil and place the above set-up into the core holder gently (to save time, you can also pure about 10 ml of hydraulic oil in the core holder before loading the set-up)

4. Tightly close the the cap of the core holder

5. Apply overburden pressure of 800 PSI

6. Connect the injection pump to one inlet of the flood-head and start the injection at a constant flowrate of 2cc/min.

7. Close the second inlet on the flood-head after you observe the water coming out of the second inlet. This is to bleed-off the air in the core holder as shown in figure E.3.

a)   b)

Figure E.4: a) Bleeding-off the air from the core holder. b) Closed flood-head

8. Observe the injection pressure on the screen of the injection pump and report it when it stabilizes.

9. Stop the injection pump

10. Unload the core sample

11. Release the overburden pressure by opening the valve on the hydraulic pump

12. Open both inlets of the flood head then open the cap.

13. To remove the sleeve along with the flood-head and end-stem, close the valve on the overburden pressure pump and pump some hydraulic oil into the core holder.

The absolute permeability to the liquid is then measured as:

$$K = \frac{14700 * Q\mu L}{A * \Delta P}$$

Where:

Q: Injection rate (ml/sec)

μ: Viscosity of the injection fluid (cP)

L: Length of the core (cm)

A: Cross Sectional area of the core (m^2)

ΔP: Pressure across the core

Example calculation (for sample 1):

$$K = \frac{14700 * (2/60)\, ml/s * 1.04cP * 5.158cm}{\frac{3.811^2}{4} * \pi\, (cm^2) * 10psi} = 23.04\, mD$$

Appendix F: IFT and Contact Angle Measurement

IFT Measurement

All Interfacial Tension (IFT) Values of oil/brine were measured by the pendant drop technique using the Teclis Tracker as shown in Figure F.1. Interfacial tension measurements are carried out at high temperature conditions using the HTHP cell provided with the instrument.

Figure F.1: Teclis Tracker instrument

The provided cell capable of withstanding high pressure and high temperature is used. The 90 °C conditions were set while maintaining the cell pressure at a maximum of 250 psia using nitrogen gas. Tracker makes use of the axisymmetric drop shape analysis (ADSA) technique to find the interfacial tension by fitting Laplace equation. The procedure followed for IFT measurements is as follows:

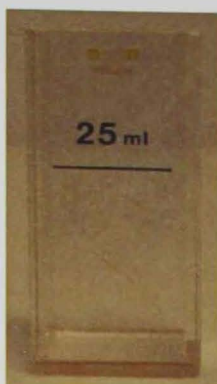1. A beaker is filled with 25ml of brine as shown in Figure F.2.

Figure F.2: Beaker of Teclis Tracker

2. The injection syringe is filled the crude oil (filtered and degasified), and U-type needle is connected to the syringe.

3. The syringe and beaker are then placed on in the stand as shown in figure F.3.a.

4. The stand is then placed in the HTHP cell (shown in figure F.3.b) and it is tightly closed.

5. The cell is placed on the pre-specified place on the instrument and the position is adjusted the position so that only the tip of the needle is shown on the camera

6. Connect the heating jackets, nitrogen cylinder and temprature probe to the cell.

7. Open the camera window with the software, and inject 2-3 drops of oil by operating the pump manually. This is to eliminate the possibility of having air bubbles in the oil drop.

Figure F.3: a) Syringe and beaker placed in the stand. b) HTHP cell

8. Open the Teclis tracker software and run the experiment after entering the exact densities of the crude oil and brine, and volume of the drop. The drop volume should be set at a volume slightly less than the intended volume to account for thermal expansion.

9. Apply the pressure of 200 psia and increase the temperature step by step up to 90°C.

10. Run the measurement until a stabilised IFT is obtained.

Contact Angle Measurements

The Teclis-Tracked instrument is used to measure the contact angle manually for 72 hours. The advantage of the following technique is that the spontaneous drainage is observed throughout the experiment. The following is the procedure for contact angle measurement:

1. The cleaned trim-ends are placed in the filtered crude oil and aged at 90°C for three weeks.

2. The aged sample is then placed in the beaker filled with brine. Make sure that there are no air bubbles on the rock surface.

3. Place the beaker and the empty syringe in the stand.

4. Place the stand inside the cell and close it tightly.

5. Adjust the position of the cell so that the camera only shows the upper surface of the trim-end.

6. Connect the heating jackets, nitrogen cylinder and temperature probe to the cell.

7. Open the Teclis tracker software, and set the setting to take pictures of the rock surface every 20-30 minutes.

8. Apply the pressure of 200 psia and increase the temperature step by step up to 90°C.

9. Monitore the contact angle for 72 hours.

Appendix G: High Temperature Spontaneous Imbibition

Ammot spontaneous imbibition tests were conducted using the HTHP cells provided by Vinci-Technologies (France) as shown in figure G.1

Figure G.1: Experimental set-up of the spontaneous imbibition

The following procedure is followed to conduct the spontaneous imbibition experiments.

1. Place the core sample in the glass container of the amott tube

2. Fill the container with brine

3. Place the graduated cylinder of the amott cell on the glass container and close it tightly using the metal clip

4. Fill the cell with brine from the top of the graduate cylinder (leave some volume for expansion of the fluids as the result of high temperature)

5. Close the cap of the graduated cylinder

6. Place the cells in the oven

7. Report the oil recovery as a function time

Appendix H: Core Flooding

Oil flooding

After brine saturation, all cores are flooded with the reservoir oil until no more formation brine is produced. At the end of the core flooding experiment, core plugs are at the initial water saturation (S_{wi}) conditions. Figure H.1 shows the PFD of oil flooding experiment.
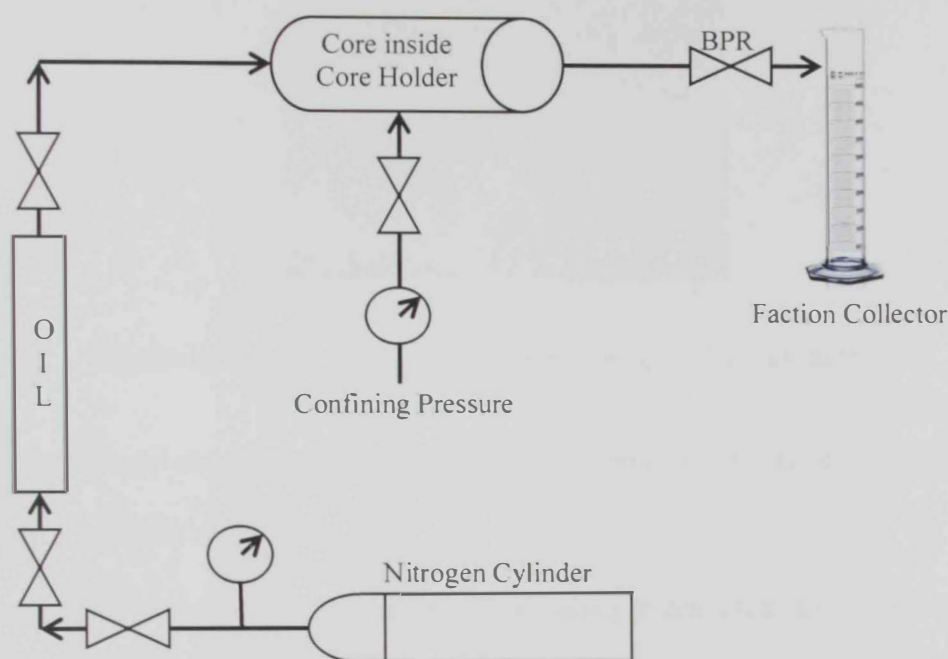

Figure H.1: Process flow diagram of oil-flooding experiment

The procedure for the oil flooding experiments is similar to the procedure explained for permeability measurement using water (Appendix E). Core flooding is conducted using the following procedure. Only differences between water-flooding and oil-flooding experiments are:

8. Gently place the core sample (at S_w of 100%) in the rubber sleeve.

9. Place the flood head at one end and the end-stem at the other end of the core, as shown in figure H.2.

10. Lubricate the end-stem with some hydraulic oil and place the sleeve into the core holder gently

11. Tightly close the Cap of the core holder

12. Apply overburden pressure of 800 PSI

13. Connect a pressure regulator valve to the end-stem as shown in figure H.2. Keep the back pressure valve closed completely.
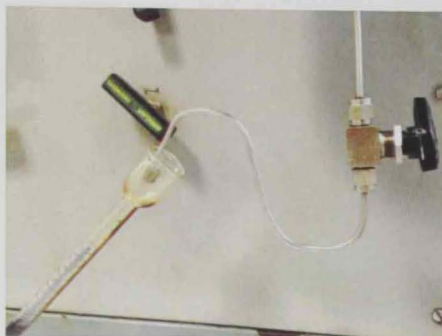

Figure H.2: Back pressure valve connected to the end-stem

14. Connect the oil container at the back of the core holder to the nitrogen cylinder and apply a pressure of 400 psig.

15. Connect the outlet of the pressurized oil container to one inlets of the flood-head.

16. Close the second inlet on the flood-head after you observe the water coming out of the second inlet. This is to bleed-off the air in the core holder as shown in figure E.4.

17. Open the oil injection valve completely while the regulator valve on the end-stem is still closed. This is to build up the pressure inside the core and ensure the flow stability.

18. Gently open the back pressure valve until a proper production rate (approximately one drop of effluent every 3 seconds) is obtained.

19. Collect the produced effluents and report the cumulative volume of the produced brine.

20. Continue the oil flood until no more brine is produced.

21. Stop the injection pump

22. Unload the core sample

23. Release the overburden pressure by opening the valve on the hydraulic pump

24. Open both inlets of the flood head then open the cap of the core holder.

25. To remove the sleeve along with the flood-head and end-stem, close the valve on the overburden pressure pump and pump some hydraulic oil into the core holder.

The initial water saturation of the core plug is calculated as:

$$S_{wi} = \frac{PV - V_{water}}{PV}$$

$$S_{oi} = 1 - S_{wi}$$

Where:

PV is the pore volume calculated using saturated weight of the core sample (Appendix D)

V_{water} is the cumulative volume of the produced brine at the end of oil flooding experiment (column 6 in table 3.5)

S_{wi} is the initial water saturation (column 7 at table 3.5)

S_{oi} is the initial oil saturation (column 7 at table 3.5)

Oil flooding experiment is usually reconducted after aging of the core plugs to evaluate any wettability alteration due to ageing. Producing more water after aging would mean that the wettability of the rock has moved toward a more oil-wetting state.

Low Salinity Water Flooding Experiments

The aged core plugs were are flooded with various brines to evaluate the effect of dilution and sulfate spiking on oil recovery. The low salinity water flooding experiments were all conducted at reservoir temperature of 255 °F (123 °C). Figure VIII.4 shows the complete set-up of LSWF experiment.
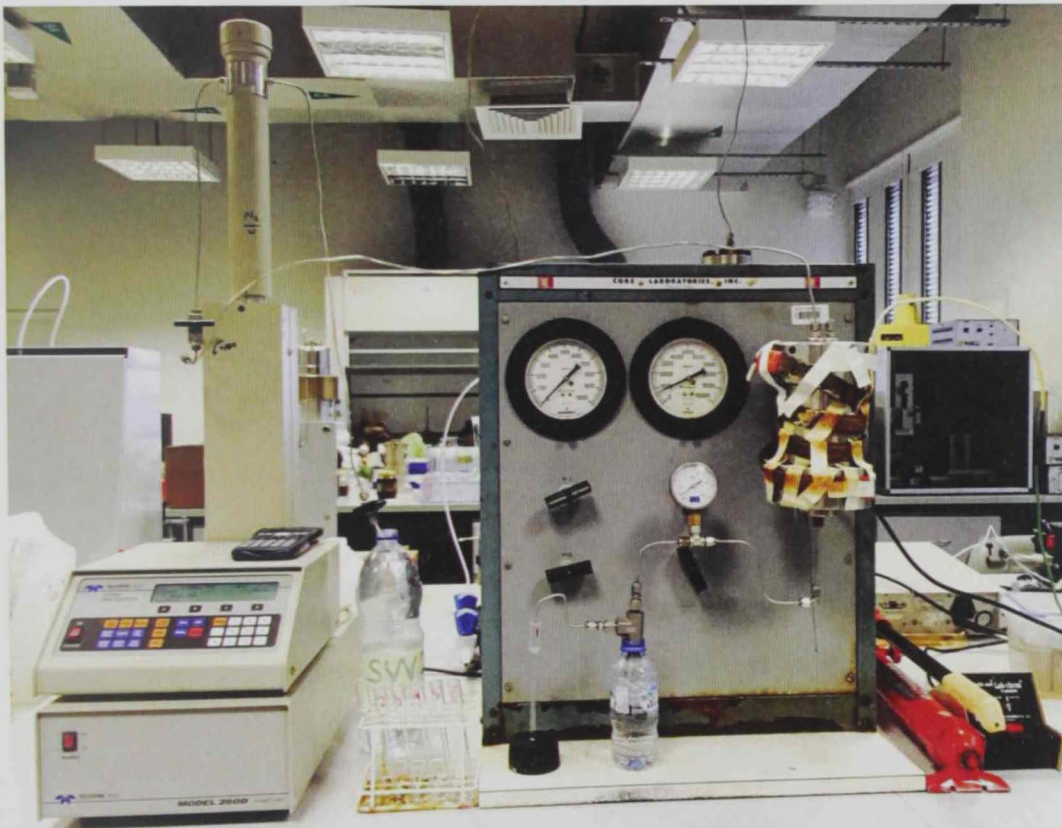

Figure H.3: Experimental set-up of the Low salinity water flooding

LSWF experiments are conducted using the following procedure.

1. Gently place the aged core sample (in S_{oi}) in the rubber sleeve.

2. Place the flood head at one end and the end-stem at the other end of the core. as shown in figure E.3.

3. Lubricate the end-stem with some hydraulic oil and place the sleeve alone with the flood head and end-stem into the core holder gently

4. Tightly close the cap of the core holder

5. Apply overburden pressure of 800 PSI

6. Adjust the back pressure regulator valve to a pressure of 150 psig, and connect to the end-stem.

7. Wrap the core holder with the heating tape and cover it with aluminum foil.

8. Increase the temperature of the core holder stepwise (steps of 20 °C)

   Note: The over burden pressure of the core holder should be continuously monitored. as the increase in the temperature results in the expanding of the hydraulic oil in the cell.

9. Fill the injection pump with the injected brine (as explained in Appendix V)

10. Connect outlet of the injection pump to one inlets of the flood-head.

11. Close the second inlet on the flood-head after you observe the water coming out of the second inlet. This is to bleed-off the air in the core holder as shown in figure E.4.

12. Operate the injection pump at the constant injection rate of 2 cc/min and start the stop watch.

13. Collect the produced effluents and report the time. the pressure and the volume of the produced oil.

14. Continue the oil flood until no more brine is produced.

15. Stop the injection pump

16. Empty and refill the pump with the next injection brine (if any)

17. Continue the flooding with the next brine at the same injection rate of 2 cc/min

18. Stop the flooding experiment when no more oil in produced.

19. Unload the core sample

20. Release the overburden pressure by opening the valve on the hydraulic pump

21. Open both inlets of the flood head then open the cap of the core holder.

22. To remove the sleeve along with the flood-head and end-stem, close the valve on the overburden pressure pump and pump some hydraulic oil into the core holder.

For every pore volume injected, the recovery factor is calculated as:

$$Recovery\ Factor = \frac{V_{oi} - V_{p.oil}}{V_{oi}}$$

Where:

V_{oi} is the volume of oil initially in place

$V_{p\ oil}$ is the cumulative volume of the oil produced at a specific pore volume injected